DEVELOPMENT OF NOVEL COLUMNS FOR DETERMINATION OF VARIOUS DIURETICS BY CAPILLARY ELECTROCHROMATOGRAPHY

A Thesis Submitted to
the Graduate School of Engineering and Sciences of
İzmir Institute of Technology
in Partial Fulfillment of the Requirements for the Degree of

MASTER OF SCIENCE

in Chemistry

by
Cemre YAŞAR

July 2018
İZMİR

We approve the thesis of **Cemre YAŞAR**

Examining Committee Members:

Prof. Dr. Ahmet E. EROĞLU
Department of Chemistry, İzmir Institute of Technology

Prof. Dr. Ali ÇAĞIR
Department of Chemistry, İzmir Institute of Technology

Assoc. Prof. Dr. Ümit Hakan YILDIZ
Department of Chemistry, İzmir Institute of Technology

Prof. Dr. Suna TİMUR
Department of Biochemistry, Ege University

Prof. Dr. Fatma Nil ERTAŞ
Department of Chemistry, Ege University

06 July 2018

Prof. Dr. Ahmet E. EROĞLU
Supervisor, Department of Chemistry
İzmir Institute of Technology

Prof. Dr. Ahmet E. EROĞLU
Head of Department of Chemistry

Prof. Dr. Aysun SOFUOĞLU
Dean of the Graduate School of
Engineering and Sciences

ACKNOWLEDGEMENTS

I would like to acknowledge the help of many people who have been there during the course of my study. Firstly, I would like to express my sincere gratitude to my advisor Prof. Dr. Ahmet E. EROĞLU for his valuable encouragement, allowing a balanced freedom to express my thoughts and improve myself throughout the study under the guidance of him.

I am also thankful to Prof. Dr. Suna TİMUR and Prof. Dr. Fatma Nil ERTAŞ who willingly accepted to be members of my thesis examining committee, Prof. Dr. Ali ÇAĞIR and Assoc. Prof. Ümit Hakan YILDIZ for their constructively suggestions and comments on this project.

I am thankful to Murat Bozkuş (Department of Administrative and Financial Affairs) for all the help in our tough times. I would like to thank Polat Bulanık and Hüseyin Bilir (Chemistry Department) for providing the chemical requirements which were a matter of urgency. I would like to thank to the research scientists at the Center for Materials Research (IZTECH) for their help on XRD and SEM. I would like to acknowledge The Scientific and Technological Research Council of Turkey (TÜBİTAK) for the support of this work through the project 205Z215.

My special thanks go to my soul sisters Esra Türker, Duygu Erdoğan and my brother Çağatay Sarıtepe; without their priceless friendship, support and encouragement everything would be harder. I wish to thank my dear friend Mustafa Umut Mutlu for his moral support and all the countless help. He is the best office-mate ever been.

I am really thankful to members of our research group especially to Merve Demirkurt Akbal and Yekta Arya Ölçer for their enlightening advices, all the help, encourage and being more than a friend. I'm so happy to be a little sister of you.

Many and deepest thanks go to my oldest friend and love of my life Barış Adalı and his beloved family (my second family) for everything that I cannot express as it should be in here.

Finally, I dedicate this work to my precious family; Akgün, Belgin, Emre Yaşar and all the other members who means too much for me and I would never be the person that I am now without have they in my corner.

ABSTRACT

DEVELOPMENT OF NOVEL COLUMNS FOR DETERMINATION OF VARIOUS DIURETICS BY CAPILLARY ELECTROCHROMATOGRAPHY

Diuretics are active pharmaceutical compounds that are used for the treatment of edema, cirrhosis, hypertension and renal failure. World Anti-Doping Agency has announced diuretics as banned compounds. Because they are used as a masking and doping agent. In this study, target compounds are therapeutically important groups of this active pharmaceuticals; namely thiazides (bendroflumethiazide, chlorothiazide, hydrochlorothiazide).

Sol-gel chemistry and molecularly imprinted polymers (MIPs) methodology were offered for preparing the column for capillary electrochromatography (CEC) for determination of thiazides. Modified silica sol-gel (amine and phenyl modified) and MIPs were synthesized through different routes (inorganic and organic form) as filling materials for capillary columns.

Materials which were filled into the column were selected by the help of sorption studies prior to CE-DAD analysis. For this purpose, critical experimental parameters of CE-DAD were optimized and determined as follows; background electrolyte type of borate buffer (10mM) and pH of 9.4, voltage of 25 kV, cassette temperature of 30°C. Limit of detection (LOD) were calculated as between 0.20 mg L^{-1} and 0.30 mg L^{-1}. Limit of quantification (LOQ) was found as between 0.44 mg L^{-1} and 0.99 mg L^{-1}.

Finally, sorbents having best sorption capacity towards the analytes were prepared as a stationary phase of capillary column and analysis was done with CEC-DAD.

ÖZET

KAPİLER ELEKTROKROMATOGRAFİ YÖNTEMİYLE ÇEŞİTLİ DİÜRETİK MADDELERİN TAYİNİ İÇİN YENİ KOLON GELİŞTİRİLMESİ

Diüretikler ödem, siroz, hipertansiyon ve böbrek yetmezliğini tedavi etmek için kullanılan aktif farmasötik bileşiklerdir. Dünya Anti-Doping Ajansı (WADA), diüretikleri yasaklı maddeler arasında yayınlamıştır. Doping maddesi olarak ve doping maddelerini maskeleyici ajan olarak kullanası nedeniyle bu listede yer almıştır. Bu çalışmada, hedef bileşikler diüretik aktif farmasötiklerin terapötik olarak önemli bir grubu olan tiazidler olarak belirlenmiştir (bendroflumetiazide, klorotiazide ve hidroklorotiazid).

Tiyazidlerin belirlenmesinde kullanılacak kapiller elektrokromatografi'nin (CEC) kılcal kolonunun hazırlanması için sol-jel kimyası ve moleküler baskılanmış polimer (MIP) metodolojisi önerilmiştir. Modifiye silika sol-jeller (amin ve fenil modifiyeli) ve farklı MIP materyalleri (inorganik ve organik formda olanlar) durgun faz olarak kullanılmak için sentezlenmiştir.

Kolon içine yüklenecek maddenin seçimi için kapiller elektroforez (CE) öncesinde sorpsiyon çalışması yapılmış. Bu amaca bağlı olarak, kritik deneysel parametreler optimize edilmiş ve tampon çözeltisi olarak 10 mM borat solüsyonu seçilip pH için 9.4 en uygun değer olarak belirlenmiş, çalışma voltajı ise 25 kV olarak, kaset sıcaklığı 30°C olarak sabitlenmiştir. Tespit limiti (LOD) 0.20 mg L^{-1} ile 0.30 mg L^{-1}, tayin limiti (LOQ) 0.44 mg L^{-1} ile 0.99 mg L^{-1} arasında bulunmuştur.

Çalışmanın sonucunda hedef bileşiklere yönelik en yüksek sorpsiyon kapasitesine sahip olan maddeler kapiller kolon içine durgun faz olarak uygulanmış ve analizler CEC-DAD ile yapılmıştır.

TABLE OF CONTENTS

LIST OF FIGURES viii

LIST OF TABLES ix

CHAPTER 1. INTRODUCTION 1

1.1. Diuretics 1

1.1.2. Thiazides and Their Metabolites 1

1.1.3. Diuretics as Doping Agents 3

1.1.4. Determination of Diuretics 3

1.2. Capillary Electrophoresis (CE) 4

1.2.1. Theoretical Background 4

1.2.2. Operation modes of Capillary Electrophoresis 8

1.2.2.1. Capillary Electrochromatography (CEC) 9

1.2.2.1.1. Stationary Phases in Capillary Electrochromatography 10

1.3. Fundamentals of Silane Chemistry and Sol-Gel 11

1.4. Molecular Imprinted Polymers (MIP) 14

Aim of This Work 15

CHAPTER 2. EXPERIMENTAL 16

2.1. Apparatus 16

2.2. Reagents and Solutions 16

2.3. Optimization of Instrumental Parameters 17

2.4. Sorbents Prepared by Sol-Gel Method 19

2.4.1. Synthesis of Silica Sol-Gel 19

2.4.2. Surface Modification of Silicate 20

2.4.3. Characterization of Sythesized Sorbents 22

2.4.3.1. Sorption Performance of Synthesized Sorbents 22

2.5. Sorbents Prepared by Molecularly Imprinting Technology 23

2.5.1. Synthesis of MIP and NIP 23

2.5.2. Synthesis of Silica Based MIIP and NIIP 24

2.5.3. Characterization of Sythesized Sorbents 25

2.5.3.1. Binding Characteristic Assay 25
2.5.3.2. Cross Sensitivity 26
2.6. Preparation of Capillary Columns 27

CHAPTER 3. RESULTS AND DISCUSSION 29
3.1. Optimization of Instrumental Parameters 29
3.2. Sorbents Prepared by Sol-Gel Method 32
3.2.1. Synthesis of Silica Sol-Gel 32
3.2.2. Surface Modification of Silicate 33
3.2.3. Characterization of Sythesized Sorbents 34
3.2.3.1. Sorption Performance of Synthesized Sorbents 34
3.3. Sorbents Prepared by Molecularly Imprinting Technology 35
3.3.1. Synthesis of MIP and NIP 35
3.3.2. Synthesis of Silica Based MIIP and NIIP 37
3.3.3. Characterization of Sythesized Sorbents 38
3.3.3.1. Binding Characteristic Assay 38
3.3.3.2. Cross Sensitivity 39
3.4. Preparation of Capillary Column 41

CHAPTER 4. CONCLUSION 43

REFERENCES 44

LIST OF FIGURES

Figure **Page**

Figure 1.1. Schematic representation of the electrical double layer at the capillary wall.....6

Figure 1.2. Schematic representation of the fractional solute migration that overall effect of electroosmotic flow and electrophoretic flow in capillary.....6

Figure 1.3. Schematic representation of capillary electrophoresis device.....7

Figure 1.4. Flow profiles in HPLC (a, c) and CEC (b, d).....9

Figure 1.5. Types of capillary columns in CEC; (a) open tubular, (b) packed, (c) monolithic. 10

Figure 1.6. Schematic representation of sol-gel method with different processing options.....11

Figure 1.7. Schematic representation of the acid and base catalyzed sol-gel processes. 12

Figure 1.8. Schematic representation of the acid catalyzed hydrolysis and condensation of silica alkoxides. 13

Figure 1.9. Schematic representation of the base catalyzed hydrolysis and condensation of silica alkoxides 13

Figure 1.10. Schematic representation of the molecular imprinting technology.....15

Figure 2.1. Schematic representation of base catalysed sol-gel process. 19

Figure 2.2. Possible (expected) shape of functionalized silicate surface after treatment with APTES, TEPS and both APTES and TEPS.....20

Figure 2.3. Illustration of the system used in hot synthesis reaction. 21

Figure 2.4. Schematic representation of MIP synthesis and template removal. 23

Figure 2.5. Schematic representation of MIIP synthesis and template removal.....24

Figure 3.1. Chromatogram of BFT (a,d), HCT (b,e) and CT (c,f) (Agilent 1200 Series HPLC-DAD system, Supelco C18 (Lichrosphere RP 18-5, 25cm×4.6mm) column, 80:20 methanol: water (acetic acid, pH 3.0) mobile phase (a, b, c), 80:20 methanol: water (phosphate buffer, pH 6.0) mobile phase (d, e, f), 0.8 mL min-^{1} flow rate) 29

Figure 3.2. Electropherogram of analytes (a) 25.0 mM borate buffer (b) 10.0 mM

borate buffer. 31
Figure 3.3. Calibration plot for bendroflumethiazide, hydrochlorothiazide and chlorothiazide. 31
Figure 3.4. SEM image of silica sol-gel. 32
Figure 3.5. SEM images of silica gel when (a) 15 mL EtOH, (b) 25 mL EtOH, (c) 45 mL EtOH, (d) 55 mL EtOH were used in the synthesis procedure. 33
Figure 3.6. SEM images of silicate with amine functional group. 33
Figure 3.7. EDX results of silicate with amine functional group 34
Figure 3.8. Sorption capacities of amine-modified, phenyl-modified, both amine-phenyl-modified and unmodified silica sol-gel particles with respect to (a) BFT, (b) HCT, (c) CT. 35
Figure 3.9. SEM images of MIP and NIP. 36
Figure 3.10. The electropherogram of BFT before and after template removal from the MIP sorbent. 36
Figure 3.11. SEM images of MIIP and NIIP. 37
Figure 3.12. The electropherogram of BFT before and after template removal from the MIIP sorbent. 37
Figure 3.13. Sorption capacities of MIP and NIP. 38
Figure 3.14. Sorption capacities of MIIP and NIIP 39
Figure 3.15. Sorption capacity of MIP and NIP in the presence of structurally related compounds. 40
Figure 3.16. Sorption capacity of MIIP and NIIP in the presence of structurally related compounds. 40
Figure 3.17. SEM image of bare silica capillary. 41
Figure 3.18. SEM image of silica capillary that was filled with unmodified silica sorbent. 42
Figure 3.19. SEM image of silica capillary that was filled with MIP sorbent. 42

LIST OF TABLES

Table **Page**

Table 1.1. Chemical structures of parent and concerned thiazides (CT, BFT, HCT) with pKa, Log K_{ow} values. 2

Table 1.2. Operation modes of capillary electrophoresis 8

Table 1.3. Stationary phases in capillary electrochromatography 11

Table 2.1. HPLC-DAD optimization parameters. 18

Table 2.2. CE-DAD optimization parameters. 18

Table 2.3. Experimental parameters related to particle size reduction. 20

Table 2.4. Experimental parameters for modified silica synthesis. 21

Table 2.5. Experimental parameters used in binding characteristic assay..... 22

Table 2.6. Experimental parameters used in binding characteristic assay..... 26

Table 2.7. Experimental parameters used in binding cross sensitivity study. 26

Table 2.8. Part I: Novel column synthesis with silicate and functionalized silicate..... 27

Table 2.9. Part II: Novel column synthesis with MIP-NIP and MIIP-NIIP 28

CHAPTER 1

INTRODUCTION

1.1. Diuretics

Diuretics are important therapeutic agents that control the reabsorption actions of electrolytes (like Na^+, K^+, H^+, Cl^-, HCO_3^- etc.) and water in the renal tubules. The main result of the controlling actions of tubular reabsorption is the increment of the urinary volume and the urinary flow rate. These pharmaceuticals are extensively used for treatment of nephropathy and also used for several disorders like cardiac insufficiencies (congestive heart failure, hypertension), cirrhosis, hypoparathyroidism, edema and diabetes insipidus (Ku Fu Hsu 2011, Goebel et al. 2004, J. Barbosa 1998, Loffing 2004).

Different chemical properties and pharmacological actions are used for the classification of diuretics. Some of the acidic diuretics are furosemide, ethacrynic acid and bumetanide which are loop diuretics. Acetazolamide (carbonic anhydrase inhibitor), trichlormethiazide, benzthiazide (thiazides) and mannitol (osmotic diuretic) are examples of weakly acidic diuretics. Also, there are some weakly basic diuretics examples from thiazide family like hydrochlorothiazide. Neutral diuretics like spironolactone and canrenone (active metabolite of spironolactone) are named as aldosterone antagonists but they belong to potassium sparing diuretics in more general respect. Basic diuretics such as triamterene and amiloride are potassium-sparing diuretics (J. Barbosa 1998, Siren et al. 2008, R. Ventura 1993, R. Ventura 1996).

1.1.2. Thiazides and Their Metabolites

Thiazides cover an entire class of fundamentally related structures that typically contain the sulfonamide group and benzothiadiazide ring (1, 2, 4-benzothiadiazine-7-sulfonamide-1,1-dioxide). Depending on the functional groups which are located in R1 R2 and R3 (Table 1.1), their relative diuretic activities, physicochemical properties and urinary excretion change (J. Tamargo 2014, R. Ventura 1996, Lemke et al. 2012).

Generally, they are eliminated from body without any change by urinary excretion, but handling the urine samples has gained importance because of hydrolysis properties of thiazides in aqueous medium which is crucial for analysis of the degradation products that will differentiate in many cases (e.g., pH, time interval, UV light exposure, temperature etc.) (Deventer et al. 2009, Goebel et al. 2004, D. Thieme 2001, Cadwallader et al. 2010).

In this study; bendroflumethiazide (BFT), chlorothiazide (CT) and hydrochlorothiazide (HCT) were investigated. Table 1.1 shows the pKa and log K_{ow} values of the related structures. Also, possible ionization sides of these molecules are indicated as amine groups which are located in sulfonamide group and embedded in benzothiadiazine ring. Chlorothiazide is the simplest form with a double bond at 3, 4 positions of parent thiazide structure and this unsaturated bond decreases the diuretic activity to 0.8 relative potency. Bendroflumethiazide and hydrochlorothiazide are saturated ones (3,4-dihydro derivatives) that are nearly 10 times more active than unsaturated forms with relative potencies of 1.8 and 1.4 respectively. Substitution of trifluoromethyl group at the 6th positions makes Bendroflumethiazide more lipid soluble than substitution of chloro groups increasing the duration of action and diuretic activity (Lemke et al. 2012).

Table 1.1. Chemical structures of parent and concerned thiazides (CT, BFT, HCT) with pKa, Log K_{ow} values.

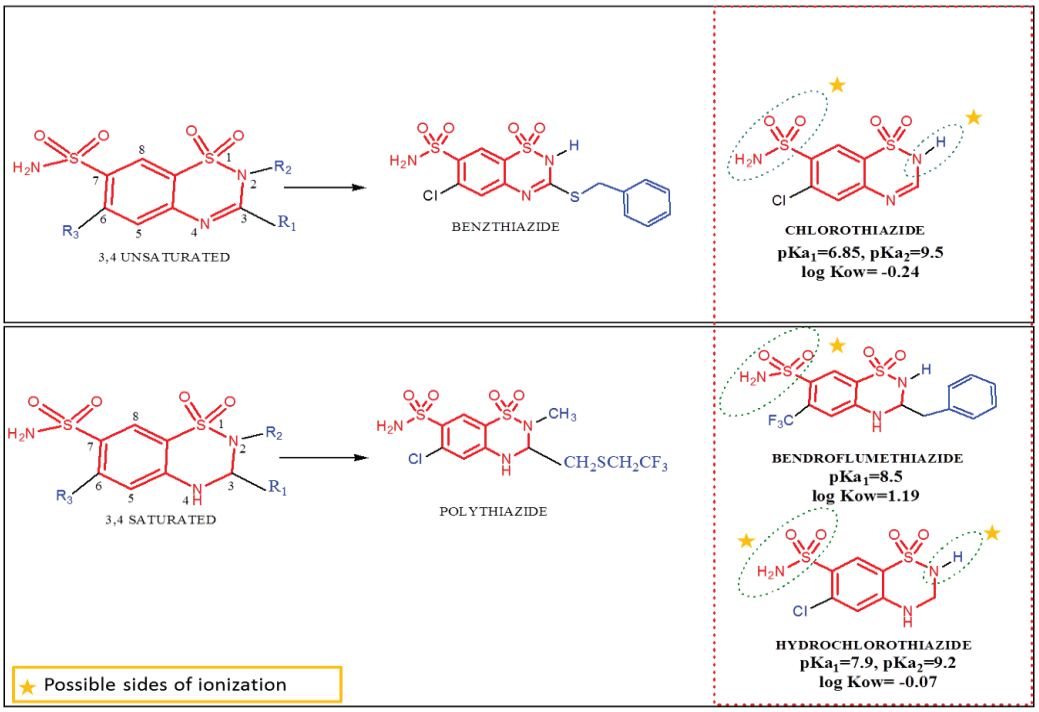

1.1.3. Diuretics as Doping Agents

International Olympic Committee (IOC) and World Anti-Doping Agency (WADA) work for the fair game in all sport competitions by the help of scientists and medical commission. List of banned substances has been revised for decades. At first it was discussed as a problem in the 1960s and best-known pioneering model about drug abuse in sport was tried at 1968 (Cadwallader et al. 2010, Botre 2008). Latest prohibited list was published by WADA at 1 January 2018 which includes ten different parent classes like anabolic agents, growth factors, hormone and metabolic modulators, stimulants, hypoxia-inducible factor (HIF) activating agents, diuretics and masking agents, β-2 agonists, etc. (WADA 2018a). Also doping control laboratories should be accredited and follow the procedure that determined by WADA, in order to get reliable results between laboratories. Minimum required performance level (MRPL) is the concept that all laboratories can reach this minimal detected concentration in their routine testing methods for non-threshold substances.

In this context, diuretics were banned in sport. They can increase urine volume and cause the alteration of urinary pH. Increasing of urine volume reduces the concentration of other doping agents and changing urine pH causes the inhibition of passive excretion actions of other illicit drugs. Also, they are stated as doping agents because of the severe weight loss actions before any competition which includes weight classes. Their MRPL was reported as 200 ng mL^{-1} at the latest reports of WADA (Morra et al. 2006, Goebel et al. 2004, R. Ventura 1996, WADA 2018b).

1.1.4. Determination Methods of Diuretics

Several methods can be found in the literature for the identification of diuretic substances in urine samples. Deventer et al. (2009) performed liquid-liquid extraction prior to liquid chromatography-electrospray ionization/tandem mass spectrometry (LC-ESI/MS/MS) and determined doping agents such as althizide, hydrochlorothiazide and their metabolites in the urine samples. In another study, Ho et al. (2013) used hollow fiber liquid-phase microextraction fibers (HF-LPME) that were immobilized with a multi-walled carbon nanotube (I-MWCNT) as sorbent. They analyzed the extracted samples by

using liquid chromatography-tandem mass spectrometry (LC-MS / MS) for eight diuretic substances and the limits of detection were determined to be in the range of 0.09 to 0.51 ng mL^{-1} (RSDs below 5.7%) for the studied diuretics. Girón et al. (2012) used ultra-high performance liquid chromatography (UPLC) and high resolution orbitrap mass spectrometry (UHPLC-HRMS) in the determination of stimulants and diuretics.

In another study, a masking agent and sixteen different diuretic substances were analyzed by using gas chromatography/electron impact-mass spectrometry (GC/EI- MS). Before the analysis, liquid-liquid extraction was used for eliminating complex matrix of urine samples then derivatization procedure (methyl derivatives are considered) was applied for GC separation (Morra et al. 2006). The limit of detections were found as 50.0 ng mL^{-1}, 20.0 ng mL^{-1}, 1.0 ng mL^{-1} for chlorothiazide, hydrochlorothiazide and bendroflumethiazide, respectively. Schappler et al. (2008) determined acidic, neutral and basic diuretic substances using microemulsion electrokinetic chromatography by hyphenated capillary electrophoresis with mass spectrometry and compared modes of screening in terms of sensitivity, selectivity and efficiency. In a relatively older study, Luis et al. (2002) used capillary zone electrophoresis (CZE) mode and micellar electrokinetic capillary chromatographic (MEKC) method for analyzing the drug mixture which include hydrochlorothiazide, furosemide, triamterene and chlorthalidone. They stated that CZE shows less efficient way for separating charged and neutral analytes than MEKC method. In addition to this, limit of detection was determined as 0.85 μg mL^{-1} for hydrochlorothiazide.

1.2. Capillary Electrophoresis (CE)

1.2.1. Theoretical Background

Capillary electrophoresis is a modern analytical method that is developed for use in the separation and determination of chemical compounds which are loaded on a buffer system and direct current is applied for movement. In this technique, there are two forces acting on the migration rates of the components; the electrophoretic effect and the electroosmotic effect.

Electrophoretic migration is based on the movement of charged particles (not neutral ones). The velocity of a charged particle (V) under electrical field is defined as in Equation 1.1 where μe is the electrophoretic mobility and E is the applied electrical field.

$$V = \mu_e \times E \quad (1.1)$$

Frictional force (F_f) and electrostatic force (F_e) are generated from the electric field and affect the electrophoretic mobility. The F_e is proportional to the applied electric field (E) and the particle charge (q), and this force is through the counter direction according to charged ion (Equation 1.2).

$$F_e = q \times E \quad (1.2)$$

The F_f tends to prevent this movement and it is expressed by Equation 1.3 (Stoke's law for a spherical ion) where ŋ is the viscosity of solution and r is the radius of ion.

$$F_f = 6.\pi.\eta.r.v \quad (1.3)$$

When these two forces reach equilibrium (Equation 1.4), ionic particles move with a constant speed.

$$q.E = 6.\pi.\eta.r.v \quad (1.4)$$

If $V = \mu e.E$ is placed into Equation 1.4 , new equation (Equation 1.5) prove the situation that electrophoretic migration rate of ions differentiate from each other depending on the charge-to-size ratio. If this ratio is large, the ion moves faster in the electric field and thus eluted earlier. The ion with a smaller charge-to-size ratio move more slowly, so eluted from capillary lastly.

$$\mu_e = q/6.\pi.\eta.r \quad (1.5)$$

Electroosmotic effect is caused by the electrical double layer which occurs between silica surface and the solution. Capillary column surface is silica (SiO_2) and above pH 3, silanol groups are deprotonated so become negatively charged. Positive ions in the buffer solution partially immobilized onto this negatively charged surface to balance it and this stationary boundary is called Stern Layer. Through the Shear Plane, voltage drops and this is called the zeta potential (ζ). The bulk solution diffuses through the capillary and as a result of the applied voltage drags all the neutral, positive and negative species which is called as electrical double. This phenomenon is presented in Figure 1.1.

The rate of electroosmotic flow is higher than the rate of electrophoretic migration. It is the main source of the moving phase in electrophoresis in the capillary column. Even if the analytes in the capillaries migrate according to their own charge-to-

size ratio, the electroosmotic flow rate is usually large enough to cause all positive, neutral and even negative species to be moved away to the same side of the capillary (Figure 1.2).

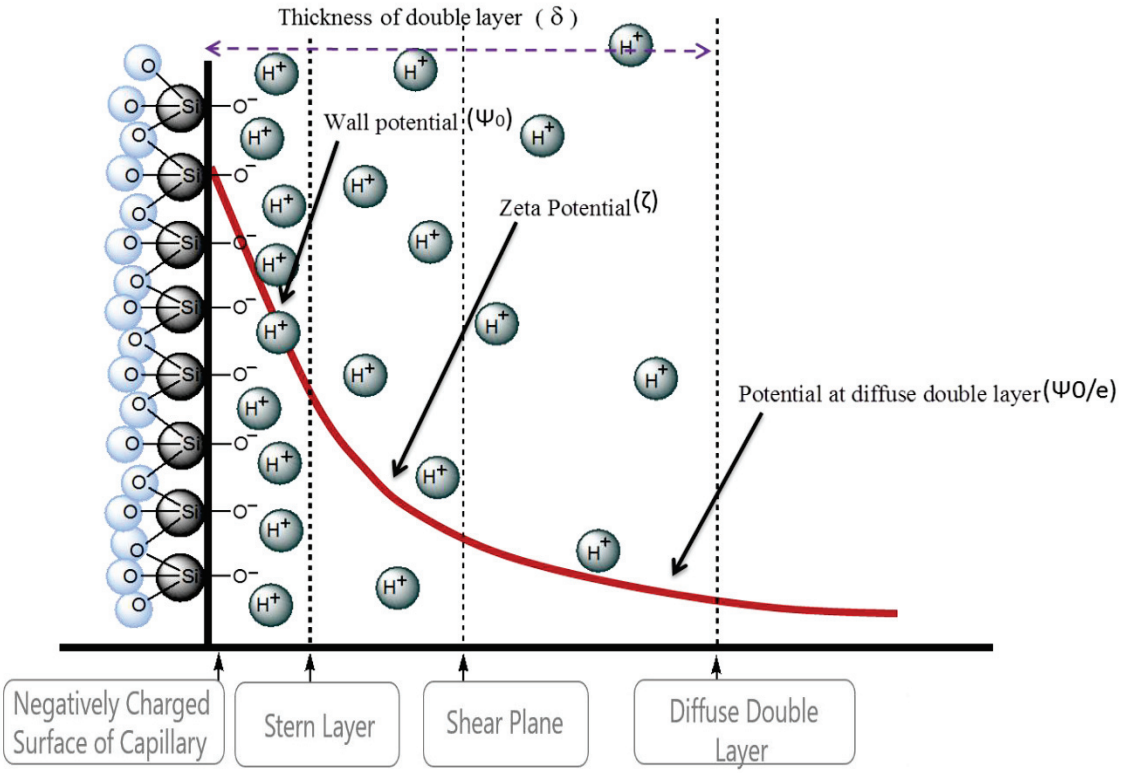

Figure 1.1. Schematic representation of the electrical double layer at the capillary wall.

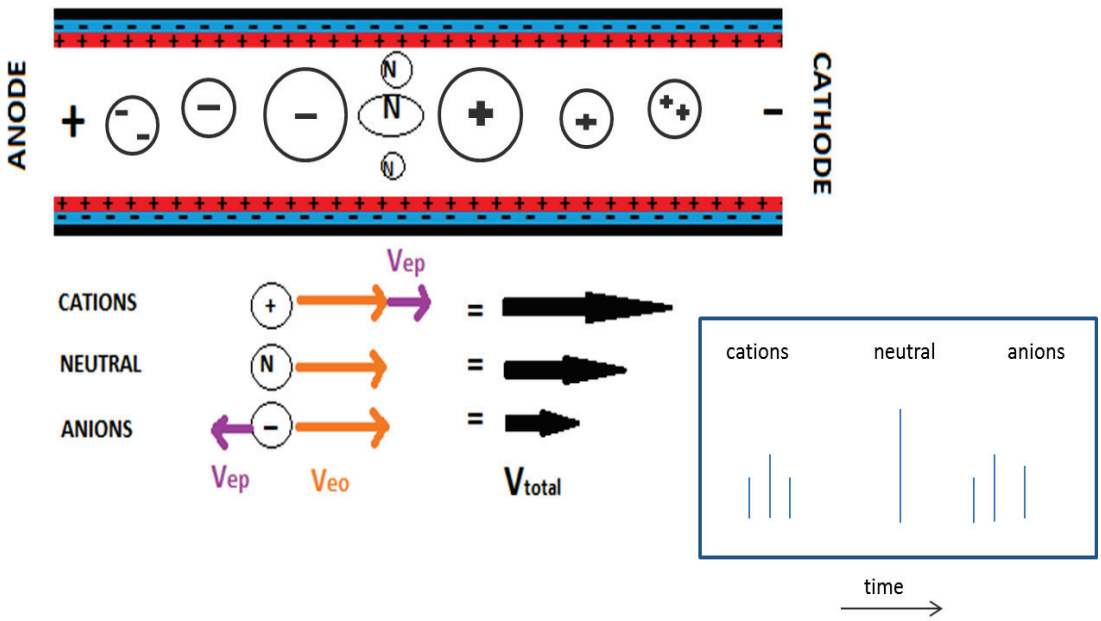

Figure 1.2. Schematic representation of the fractional solute migration that overall effect of electroosmotic flow and electrophoretic flow in capillary.

The resulting electropherogram is similar to the chromatogram (Figure 1.2). In that case, the velocity (V total) of an ion is the sum of its electrophoretic flow (EPF) velocity (Equation 1.6) and its electroosmotic flow (EOF) velocity. Equation of electroosmotic mobility also shown as below where ζ is the zeta potential (Equation 1.7)

$$V_{total} = (\mu_e + \mu_{eo}).E \quad (1.6)$$

$$\mu_{eo} = \varepsilon.\zeta/\eta \quad (1.7)$$

There are several factors affecting the electroosmotic flow that should be optimized for an analysis, e.g. electrical field, pH of buffer, temperature (effect the viscosity of solution), coating of the capillary wall (it can increase or decrease the EOF or change the flow direction and also eliminate the EOF), addition of organic modifiers and surfactants (Agilent Technologies 2014, Jiskra 2002).

Capillary electrophoresis (CE) allows the analysis of a wide range of proteins, drugs, inorganic cations and anions, carbohydrates, polynucleotides, nucleic acids, amino acids, vitamins, peptides, etc... It has some advantages such as working with small volume of samples (approach of green chemistry), simple instrumentation, cheap and durable capillary columns, high separation efficiency and quick separations according to other methods used in the industry (Siren et al. 2008, Alnajjar et al. 2013, Pena Crecente et al. 2016, Kitagawa and Otsuka 2011, Kasicka 2012, Tang et al. 2014, Eeltink and Kok 2006).

A simple CE system consist of a sample vial, inlet and outlet vial which contain background electrolyte (buffer solution), capillary, detector (UV-Vis, DAD, Laser Induced Fluorescence, Contactless Conductivity Detection, etc.), high voltage supplier and computer (Figure 1.3) (Agilent Technologies 2014).

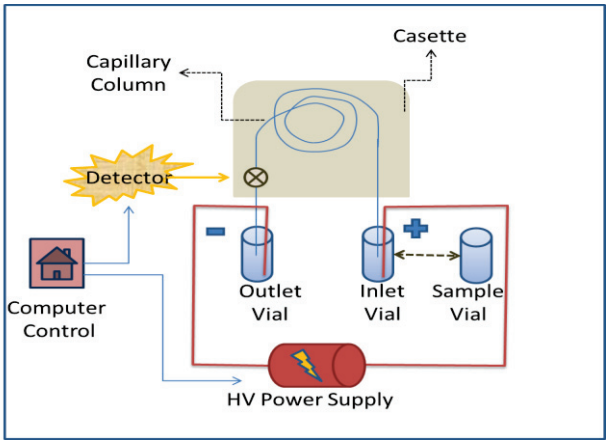

Figure 1.3. Schematic representation of capillary electrophoresis device.

1.2.2. Operation modes of Capillary Electrophoresis

Capillary electrophoresis operation modes show differences according to the separation principles that they depend on. Generally, changing the buffer composition or supporting material of inner capillary helps accessing of different modes of action (Table 1.2) (Agilent Technologies 2014). In this study, capillary electrochromatography mode was chosen for the determination of diuretics. Its prominent features like high efficiency, rapid separation and comparability of the electrochromatogram with similar techniques make it an attractive option for analysis. All these features are discussed in the following section.

Table 1.2. Operation modes of capillary electrophoresis

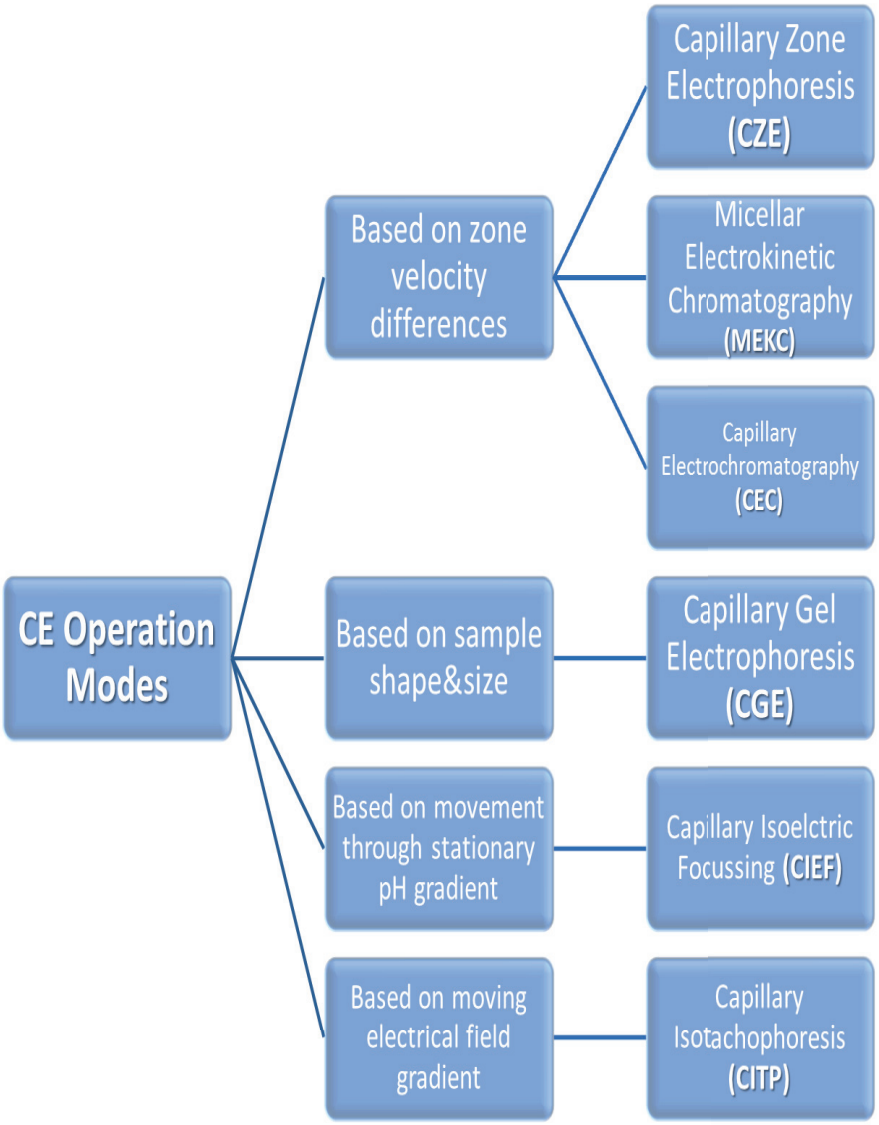

1.2.2.1. Capillary Electrochromatography (CEC)

Capillary electrochromatography is a mixed method based on a basic chromatographic theory and capillary electrophoretic methodology. Separations of analytes are achieved by the help of both electrophoretic mobility and partition of analytes between mobile phase and stationary phase or by only one of these phenomena. In CEC mode, electrical force is applied like in the CE mode, but at this time, capillary column has a stationary phase in it. The technique is very similar to the CE, so only a few additions (external pressure system and specified capillary) to the CE device make possible the CEC analysis. Unlike HPLC which has a parabolic flow shape, CEC has a flat-like flow shape in column which reduces the plate height and increases the separation efficiency compared to HPLC (Figure 1.4). Increasing the column length causes higher the pressure and also decreases speed of analysis in HPLC. However, in CEC electro-driven forces do not depend on the column length, so longer columns can be used if needed. Particle diameter is important in pressure-driven flow. Because the path, through which solution flows, can be changed for the analyte molecules which causes zone broadening. However, in electro-driven case flat-like flow profile prevents this zone broadening and back pressure (Smith 1999, Agilent Technologies 2014, Jiskra 2002, Eeltink et al. 2003).

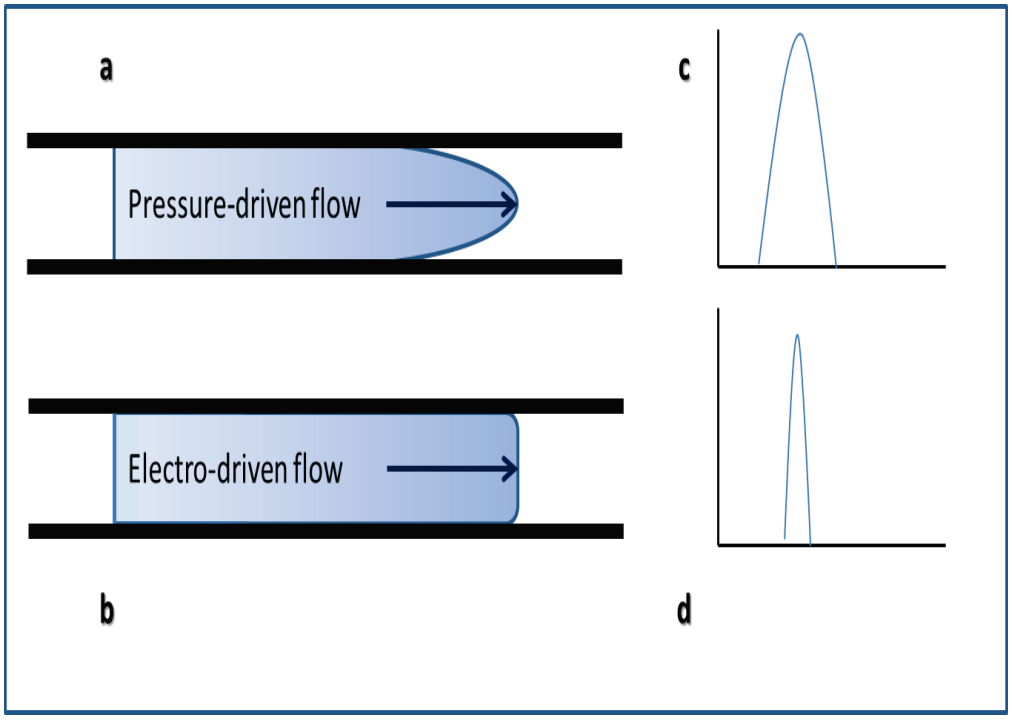

Figure 1.4. Flow profiles in HPLC (a, c) and CEC (b, d).

1.2.2.1.1. Stationary Phases in Capillary Electrochromatography

The technology of column development in capillary electrochromatography was simply begun with the usage of stationary phases of commercial HPLC columns. In that case, stationary phases were ineffective to create durable and strong electroosmotic flow under applied background electrolyte. So, many methods have been evolved in the way of generating required EOF.

In morphological perspective there are three type of columns; open-tubular, monolithic and packed (Figure 1.5).

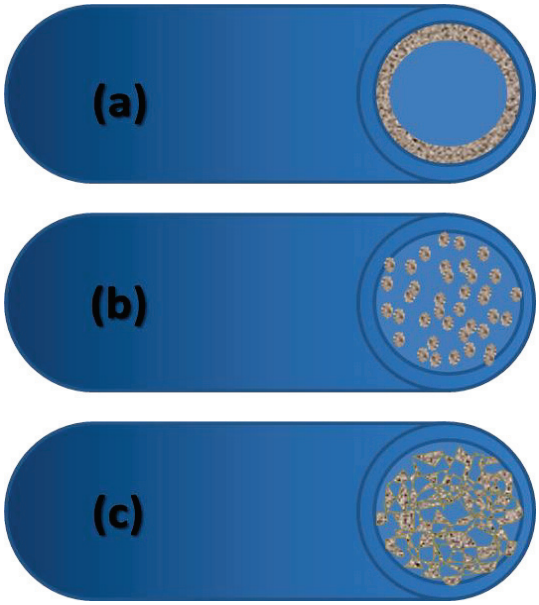

Figure 1.5. Types of capillary columns in CEC; (a) open tubular, (b) packed, (c) monolithic.

Materials used in the preparation of stationary phases are divided in two main categories; polymer based (organic) and silica based (inorganic) stationary phases (Table 1.3). Preparation of stationary phase requires a well-organized procedure to satisfy the expectations of analysis. Both surface chemistry and porosity should be taken into account. Lots of filling types were reported in literature that depends on specific purposes like; chiral separation, ion-exchange, hydrophilic or hydrophobic partition, ligand selective, normal or reverse phases, etc.(Jiskra 2002, Cheong et al. 2013, K.D. Bartle 2000, Tarongoy et al. 2016, M. Ganzera 2010, Eeltink et al. 2006, Eeltink et al. 2003).

Table 1.3. Stationary phases in capillary electrochromatography.

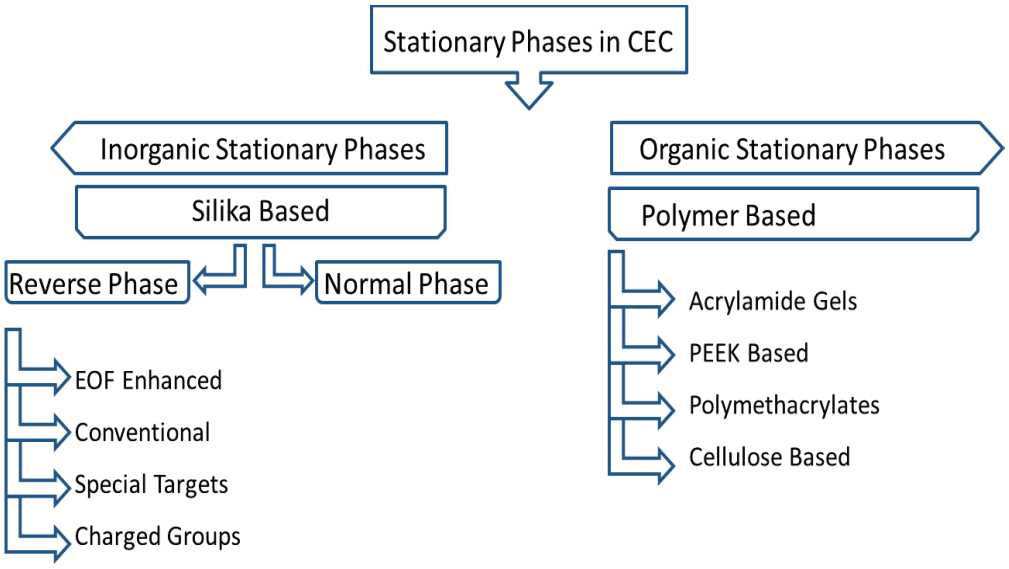

1.3. Fundamentals of Silane Chemistry and Sol-Gel

The sol-gel technology involves generating 3D oxide network in a liquid phase by growing polycondensation of the sol precursors. The desired final form is constituted by removal of the solvent with different types of methods which are represented in Figure 1.6 (Schubert et al. 2000).

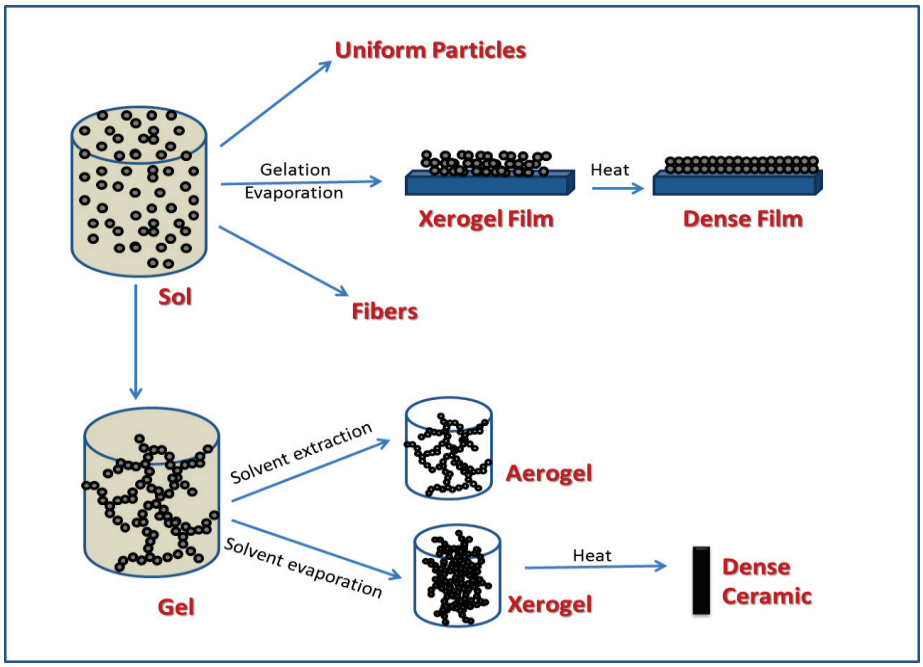

Figure 1.6. Schematic representation of sol-gel method with different processing options.

Sol-gel method is a very worthwhile technique for obtaining both inorganic and organic-inorganic hybrid polymers. The entire process is carried out on very mild conditions and that is the main advantage of this technique. Unlike the solid state processes, the sol-gel technique allows controlling the reaction at molecular level during the transition of the precursor species to the final product. Hence, the synthesis of highly pure, homogeneous and well-defined nanoparticles with uniform crystal structure can be obtained (Schubert et al. 2000, L. Hench et al. 1990, Danks et al. 2016).

Firstly, homogeneous solutions of very pure starting materials are prepared. Then hydrolysis is carried out by adding water to alkoxide solution. The reaction was catalyzed under basic or acidic conditions to provide polycondensation of the hydrolyzed monomers. In the acid catalyzed mechanism, a linear or randomly branched polymer is formed. At an equal catalyst concentration, the base catalyzed reactions are slower than the acid catalyzed reactions. Also, the structure of the product is in more condensed form (Figure 1.7). Sol-gel structure occurs as a result of the peptization. Hydrolysis and condensation reactions make the sol highly viscous until the gel is formed. The gel can be imagined as a porous 3D-web in the liquid. Sol-gel contains substances in side this 3D-web; such as alcohol and water. For final form; it can be heated to remove water, organic solvents, etc…

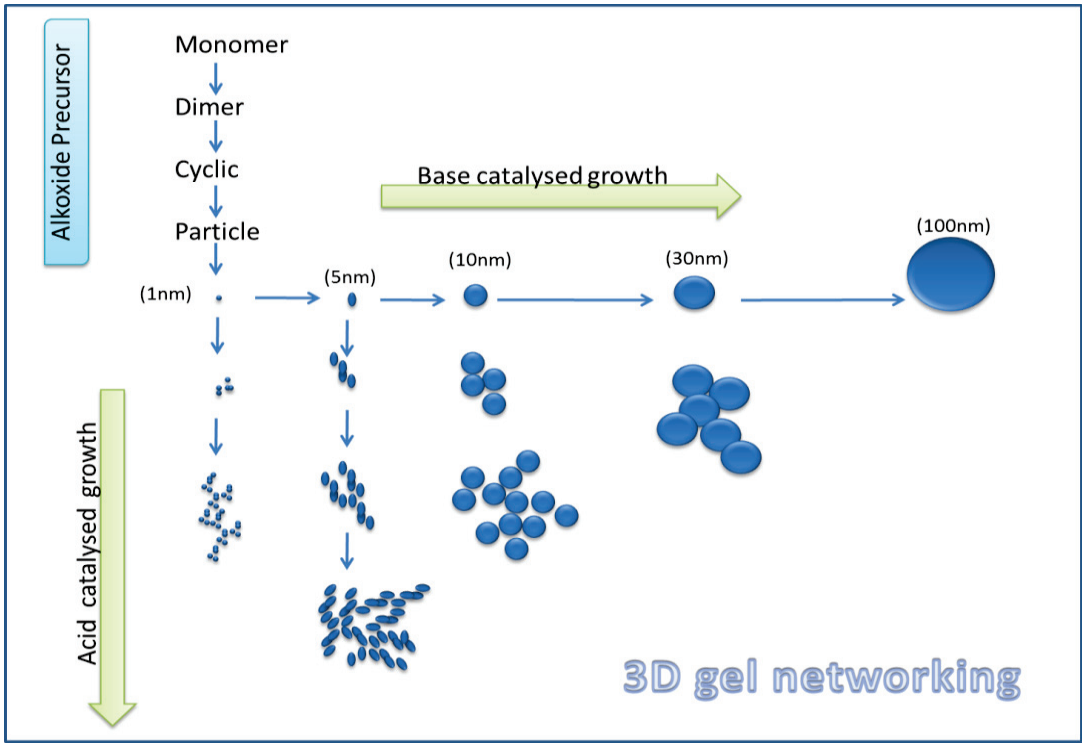

Figure 1.7. Schematic representation of the acid and base catalyzed sol-gel processes.

The initial alkoxide species have significant effects on the reaction. The fine particles tend to reduce active surface area (minimizing the energy of the system), and agglomeration occurs. To prevent this phenomenon, repulsive force effect and steric barrier are needed. The silicon compounds have generally four coordination numbers, but it is not convenient for the nucleophilic attacks. Stability of silicates are high enough to easily handle it. Also silica alkoxides provide the steric barrier and electrostatic repulsion that are important for sol-gel procedure. The representations of hydrolysis and condensation mechanisms of silica under acidic and basic conditions are given in Figure 1.8 and 1.9, respectively (Danks, Hall, and Schnepp 2016, Schubert and Hüsing 2000, Larry L. Hench 1990).

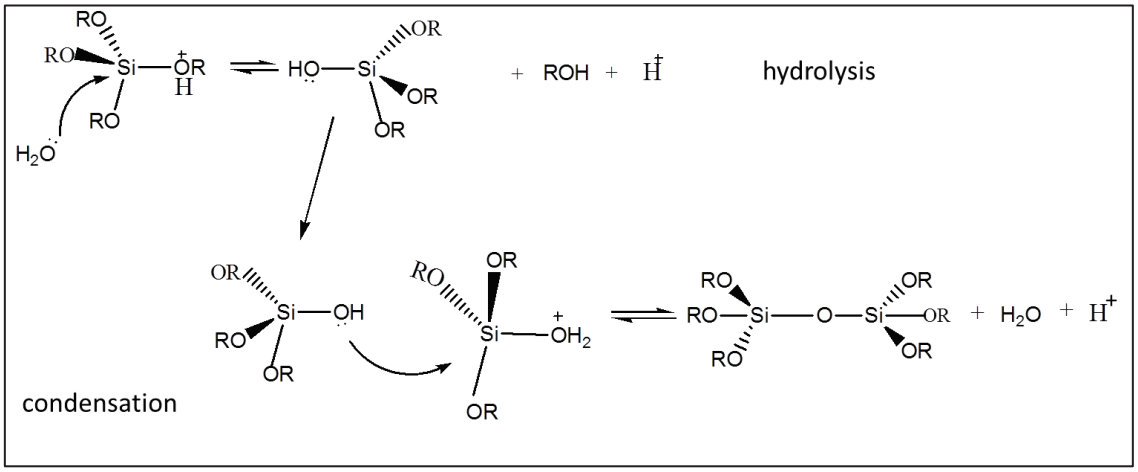

Figure 1.8. Schematic representation of the acid catalyzed hydrolysis and condensation of silica alkoxides.

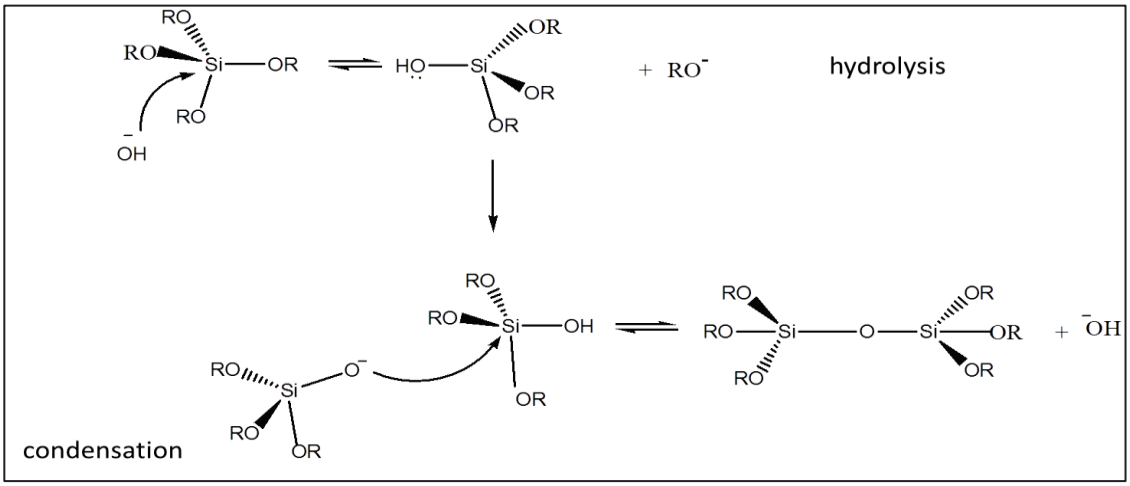

Figure 1.9. Schematic representation of the base catalyzed hydrolysis and condensation of silica alkoxides.

1.4. Molecular Imprinted Polymers (MIP)

The molecular imprinting methodology is an attractive way to design highly specific materials in molecular manner for sorption, determination or detection the analytes. Many advantages like low production cost, good mechanical and chemical stability, selectivity and biocompatibility make this technology highly favorable. Applications of inorganic or organic branches of molecular imprinting technology are used in a wide range of fields like stationary phases of chromatographic methods, antibody-antigen system mimicking, solid phase extraction sorbents, drug delivery systems, sensors etc.(Chun Deng 2015, Iacob et al. 2014, Junjie et al. 2013, Lv et al. 2012, Mu et al. 2015).

Basically, imprinting technology work on a knitting polymer network around the template molecule with monomers and reinforcing the structure with cross linkers. The template molecule and monomer interact with each other (semi-covalently or non-covalently), breaking these interactions let the template removal. The resulting structure has cavities that are specific to template molecule. Hence, these molecularly imprinted polymers (MIPs) tend to interact with the template molecule and all the other structurally related ones. Non-imprinted polymers can be imagined as the blank of the MIPs, since template molecule is not used in this case and all the steps remains same. Because the special cavity does not occur, selectivity towards the analyte not expected. Schematic representation of the steps is given in Figure 1.10 (Sellergren 2000, Sarafraz-Yazdi et al. 2015, Olcer et al. 2017).

Molecularly imprinted materials can be synthesized by using organic or inorganic precursors. Also, it can be hyphenated as organic-inorganic imprinting. In that case purpose of the experiment must be determined carefully. For example; organic based MIPs show excellent stability towards pH changes but swell or shrink upon exposure to different kinds of solvents. But the polymerization process of this type of MIPs is more easily controlled than inorganic ones. In the perspective of inorganic based MIPs, they show high stability towards solvent and mechanical strength for swelling or shrinkage. However, controlling the polymerization is more complex and need of post-modifications makes it less desirable. Thus, hybrid of these two materials can be composed of and adsorption capacity, mechanical strength, reaction pathway can be adjusted (Wu et al. 2011, Lv et al. 2012, Mu et al. 2015, Huang et al. 2009, Junjie et al. 2013, Ou et al. 2015).

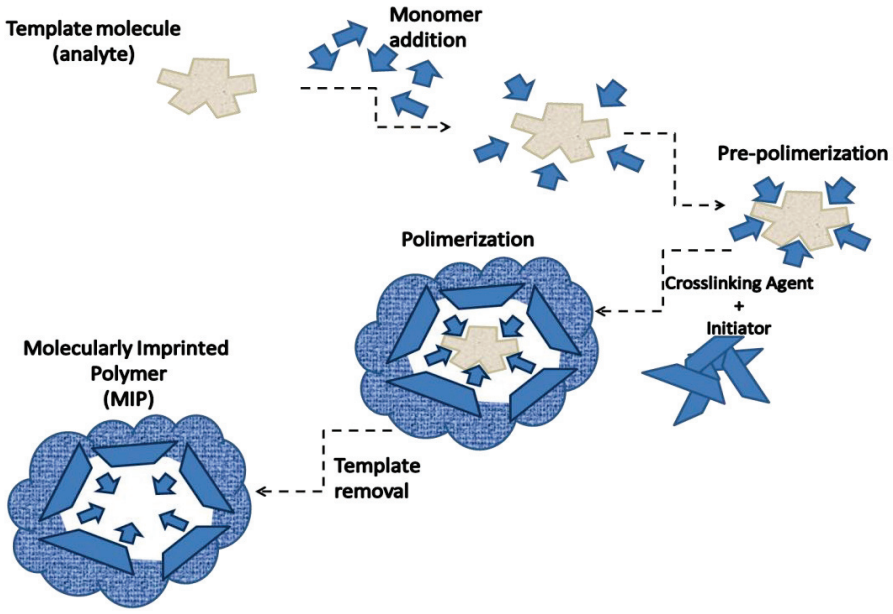

Figure 1.10. Schematic representation of the molecular imprinting technology.

Aim of This Work

The main objective of this study is to develop novel columns for the selective determination of thiazides (diuretics) by capillary electrochromatography. The packing materials were synthesized by following two different methods. Sol-gel technique was one of the methods for the synthesis of silica and functionalized silica (with amino and phenyl groups) stationary phases. Molecularly imprinting method was used for the generation of both organic stationary phase (MIP) and inorganic stationary phase (MIIP). All the synthesized packing materials were investigated in terms of binding ratios by running out the sorption studies prior to CE-DAD. The experimental parameters for CE-DAD were optimized; these were concentration, pH, and type of the buffer solution, injection parameters (pressure, voltage and time), column temperature, voltage. According to the results of sorption performances, one of the synthesized materials was chosen for each category and capillary column was packed with them. The coating layer number of stationary phases, method for injection of stationary phase into capillary and places that reaction started were changed and optimized. To make an orthogonal analysis HPLC-DAD study was carried out.

CHAPTER 2

EXPERIMENTAL

2.1. Apparatus

Samples were analyzed by using a UV-Vis Spectrometer (Varian Cary 50 scan), Agilent 1200 series HPLC equipped with Diode Array Detector (DAD) (Agilent Technologies, USA). Supelco C18 (Lichrosphere RP 18-5, I.D.:250mm×4.6mm) analytical column was used for HPLC. Agilent 7100 series CE equipped with DAD used as Capillary Electrophoresis. Agilent Technologies undeactivated fused capillaries were used (id. 50 μm or 75 μm). Quanta 250FEG Scanning Electron Microscope (SEM) and Philips X'Pert Pro X-Ray Diffractometer (XRD) were used for characterization.

Hettich EBA 12 centrifuge (Tuttlingen, Germany) was used for the separation of sorbent in some cases. Elmasonic S 80 H was used for the ultrasonication. Adjustment of the solution pH was performed by using Ino Lab Level 1 pH meter (Weilheim, Germany). A basic orbital shaker, IKA yellow line OS 5 (Staufen, Germany) was used for mixing. Ultra-pure water (18.2 MΩ, Millipore, Billerica, MA, USA) was used throughout the study.

2.2. Reagents and Solutions

Bendroflumethiazide (99%, BFT), Hydrochlorothiazide (99%, HCT), Chlorothiazide (99%, BP), Methanol (99.9%MeOH), Ethanol (99.8%, EtOH), Acetonitrile (99.9%, ACN), Tetraethoxysilane (98%, TEOS), 3-Aminopropyl-triethoxysilane (97%, APTES), Triethoxyphenylsilane (98%, TEPS), 3-(Trimethoxysilyl)propyl methacrylate (98%, TMSPMA), Methacrylic Acid (99%, MA), Ethylene glycol dimethacrylate (98%, EGDMA), Potassium Phosphate Monobasic (99%, KH_2PO_4), Potassium Phosphate Dibasic (98%, K_2HPO_4) were obtained from Sigma-Aldrich (St. Louis, MO, USA). Ammonium hydroxide solution (%25, $NH_3.H_2O$), Glacial Acetic Acid (100%, HOAc), Tetrahydrofuran (99.9%, THF), di-Sodium tetraborate

decahydrate ($Na_2B_4O_7{}^*10H_2O$), Acetone, Silica gel 60 (0.2-0.5mm) were purchased from Merck (Darmstadt, Germany). Toluene was obtained from Riedel de-Haen. 4,4′-Azobis (4-cyanovaleric acid) (AIVN) were obtained from Alfa Aesar (Haverhill, Massachusetts, USA).

All chemicals were of analytical reagent grade and ultrapure water was used throughout the study (UPW, 18.2 MΩ, Millipore, and Billerica, MA, USA). Adjustments of the pH were done by using different concentration of NaOH-HCl (0.01 M, 0.1 M, and 1.0 M) solutions. Plastics and glassware were washed firstly with detergent and then acetone, finally with ultrapure water prior to use.

Stock solutions of BFT, HCT and CT (1000.0 mg L^{-1} and 100.0 mg L^{-1}): prepared by dissolving in HPLC grade methanol (MeOH) separately and stored in amber bottles at – 4 °C in refrigerator. Lower concentration of standard solutions were prepared freshly by appropriate dilution of stock solutions. Sample solutions were filtered by using polyamide or cellulose acetate membrane (0.25 μm) depending on the solvent system.

2.3. Optimization of Instrumental Parameters

Bendroflumethiazide, hydrochlorothiazide and chlorothiazide stock solutions (100.0 and 1000.0 mgL^{-1}) were prepared in methanol and stored in 4 ˚C at refrigerator.

The tested HPLC-DAD parameters are shown in Table 2.1. Limit of detection (LOD) and limit of quantification (LOQ) were not calculated for HPLC because of the failure in peak separation and correction.

The tested CE-DAD parameters are shown in Table 2.2. Before each run a settled conditioning method was applied to the capillary column. Conditioning steps are;

1. Wash with MeOH for 5 min
2. Wash with UPW for 5 min
3. Wash with 1M NaOH for 5 min
4. Wash with 0.1M NaOH for 5 min
5. Wash with UPW for 5 min
6. Wash with Buffer for 5 min.

Also, the pre-conditioning steps were repeated after every 4 injections to ensure the repeatability.

Table 2.1. HPLC-DAD optimization parameters.

Column	Supelco C18 (250 mm x 4.6 mm) column
Mobile phase	80:20 methanol:water (acetic acid, pH 3.0) 80:20 methanol:water (phosphate buffer, pH 6.0)
Thermostat temperature	30.0 ºC
Sample injection volume	20.0 µL
Standard solutions	1.0, 5.0, 10.0, 20.0 mgL^{-1}
Flow rate	0.7, 0.8, 0.9 $mLmin^{-1}$

Table 2.2. CE-DAD optimization parameters.

Column	Agilent Technologies, FS, Undeactivated (50 µm i.d. column)
Casette temperature	25.0, 30.0 º C
Injection pressure	50.0, 60.0 mbar
Injection time interval	5.0, 10.0 sec
Power & Current	6.0W, 300µA
Voltage	10.0, 15.0, 20.0, 25.0, 30.0 kV
Peak width	0.31, 0.62, 1.25, 2.5, 5.0 Hz
Electrolyte solution	25.0 mmol Borate Buffer (pH 9.3), 10.0 mmol Borate Buffer (pH 9.2, 9.3, 9.4, 9.5) 25.0 mmol Phosphate Buffer (pH 7.0)
Timeable function	Off and 6.8 /6.7 /6.6 s change voltage to 15kV
Standard solutions	0.5, 1.0, 5.0, 10.0, 20.0, 25.0, 50.0, 100.0 mgL^{-1}

Limit of detection (LOD) and limit of quantification (LOQ) were calculated by analyzing the least concentrated standard 10 times with CE-DAD.

2.4. Sorbents Prepared by Sol-Gel Method

2.4.1. Synthesis of Silica Sol-Gel

Synthesis of silicate structures was carried out using the sol-gel route with slight modifications of the method described by Strandwitz et al. (2009).

First, the alkoxide solution was prepared using 1000.0 μL TEOS and 35.0 mL EtOH. While stirring this mixture by magnetic stirrer at 500 rpm, the base catalyst solution was added to initiate gelation (Fig. 2.1). This catalyst solution contains 7.0 mL of deionized water and 1.05 mL of ammonium hydroxide (25%, NH_4OH). Reaction takes place at room temperature (24 hour). The excess solution was removed with successive centrifugation of the mixture for 30 min at 6000 rpm. Then redispersion was applied by using (50:50) $_dH_2O$: EtOH mixture and centrifuged again (6000 rpm, 10 min). Last redispersion was applied with deionized water and centrifuged at 6000 rpm for 10 min. The resulting silicate nanoparticles were dried at 50.0 ºC, overnight in an oven. The amount of solvent (EtOH) and the amount of TEOS, which is a silica source, were changed to obtain different nano-sized structures (Table 2.3).

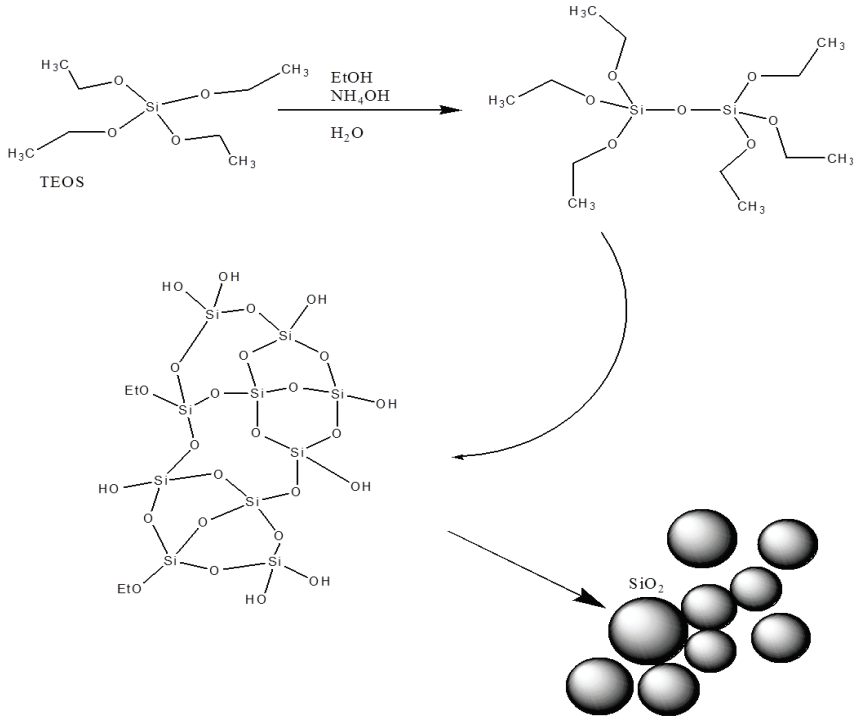

Figure 2.1. Schematic representation of base catalysed sol-gel process.

Table 2.3. Experimental parameters related to particle size reduction.

	TEOS	EtOH	Deionized water	$NH_3.H_2O$
1.(reference point)	1000 µL	35 mL	7 mL	1.05 mL
2.trial	750 µL	35 mL	7 mL	1.05 mL
3.trial	500 µL	35 mL	7 mL	1.05 mL
4.trial	250 µL	35 mL	7 mL	1.05 mL
5.trial	100 µL	35 mL	7 mL	1.05 mL
6.trial	1000 µL	15 mL	7 mL	1.05 mL
7.trial	1000 µL	25 mL	7 mL	1.05 mL
8.trial	1000 µL	45 mL	7 mL	1.05 mL
9.trial	1000 µL	55 mL	7 mL	1.05 mL

2.4.2. Surface Modification of Silicate

It is expected that the π-π stacking interaction, H-bonding and the polar-polar interactions play an important role in holding of analytes to the surface. In order to create H-bonding and π-π stacking, the silica surface was functionalized first with 3-aminopropyltriethoxy silane (3-APTES) and then triethoxyphenylsilane (TEPS). For comparison, they were also added at the same time (Fig.2.2).

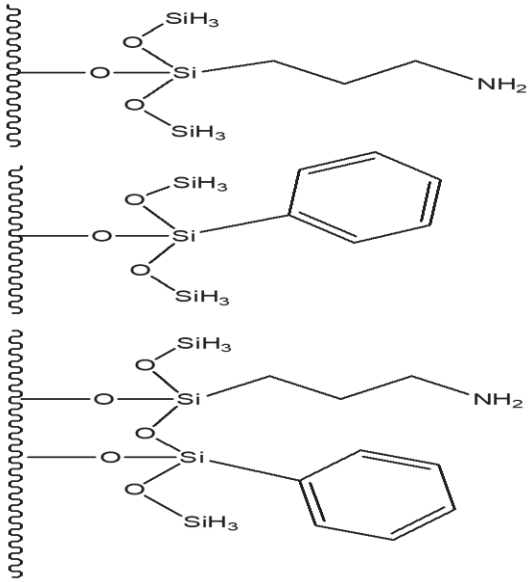

Figure 2.2. Possible (expected) shape of functionalized silicate surface after treatment with APTES, TEPS and both APTES and TEPS.

Surface modification was done by utilizing and modifying the literature knowledge (Boyaci et al. 2011). The surface of the newly synthesized nanosilica gel particles was activated in 10 mL deionized water with 0.01M acetic acid by stirring them for an hour. Then the washing step was applied with deionized water until pH was neutral. Activated silica nanoparticles were dried for 24 hours at 120 ºC then placed in the reaction vessel (Figure 2.3). TEPS molecules and APTES were bonded to the surface by hot synthesis. For this purpose, 10 mL of toluene, activated silica particles and TEPS and APTES used for modification. They were mixed in the reaction flask at 100 rpm in oil bath and heated up to 90 ºC under Ar gas. Meanwhile, two condenser system and $CaCl_2$ drying agent was on top of the system.

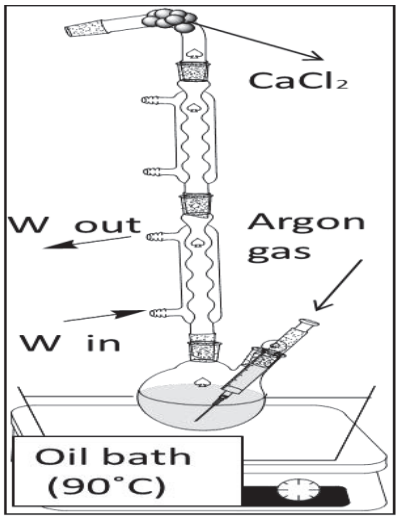

Figure 2.3. Illustration of the system used in hot synthesis reaction.

In the experiments, parameters such as temperature and solvent amount were kept constant. Abbreviations and ratios of synthesized and modified silica materials are given in Table 2.4.

Table 2.4. Experimental parameters for modified silica synthesis.

Synthesized surface	Silica nanoparticle (g)	Acetic acid (µL)	APTES (mL)	TEPS (mL)
APTES-SiO_2	1.50	8.40	0.9	x
TPES-SiO_2	0.50	2.80	x	0.3
A-P-SiO_2	1.50	8.40	0.45	0.45

2.4.3. Characterization of Sythesized Sorbents

Images of silicate, functionalized silicate nanoparticles and filled capillaries were taken with scanning electron microscopy (SEM) to realize the morphologies of synthesized materials and prove the filling of capillary.

Firstly, the selectivity of the synthesized materials to diuretic drugs was tested by solid phase extraction (SPE) method prior to CE. Further capillary filling experiments were continued with materials that give satisfactory results in sorption performance.

2.4.3.1. Sorption Performance of Synthesized Sorbents

Sample solutions were prepared as in Table 2.5. Sorbents (amine modified silicate, phenyl modified silicate, amine and phenyl modified silicate and unmodified silicate) were added into 10.0 mL of sample solutions and shaken at 480 rpm for 24 hours. After, the mixture was filtered through filter tip cellulose acetate or polyamide membranes (0.2 μm pore size) to separate sorbents from solutions. Effluents were analyzed by CE-DAD using 10.0 mmol borate buffer (pH 9.4).

Table 2.5. Experimental parameters used in binding characteristic assay.

Standard concentrations of BFT, HCT, CT mixture	0.5, 1.0, 5.0, 10.0, 25.0, 50.0, 100.0 mgL^{-1}
Amount of sorbent	10.0 mg
Sample solution volume	10.0 mL
Sorption time	24 hour
Shaking speed	480 rpm
Ambient temperature	25.0˚C

2.5. Sorbents Prepared by Molecularly Imprinting Technology

2.5.1. Synthesis of MIP and NIP

Molecularly imprinted polymer (MIP) and its blind (non-imprinted polymer, NIP) were synthesized as various solid phase extraction (SPE) sorbents for the selected template molecule (bendroflumethiazide, BFT) to increase the selectivity through the thiazide family prior to CE analysis. A schematic of the MIP synthesis in which BFT is selected as template molecule is given in Figure 2.4. Polymerization reaction includes methacrylic acid (MA) as monomer, ethylene glycol dimethyl methacrylic acid (EGDMA) as crosslinker, 4,4'-azobis(4-cyanovalericacid) (AIVN) as initiator and acetonitrile as solvent. Firstly, in the pre-polymerization step of MIP; $1x10^{-4}$ mmol BFT and 10 mL acetonitrile were stirred in an amber rounded bottom flask for 30 min. Then $4x10^{-4}$ mmol MA was added to flask and stirred for 1.0 hour. Then, $20x10^{-4}$ mmol EGDMA was added to the flask under Ar gas (to remove oxygen) and after 5 min, AIVN (% 2.0 mole of monomer and crosslinker) was added. Ar gas was kept bubbling about 10 min. Reaction was performed in an inert medium and temperature was kept constant at 60ºC by the help of oil bath (420 rpm, 24 hours). In NIP case, all steps were kept the same, just BFT was excluded from reaction procedure.

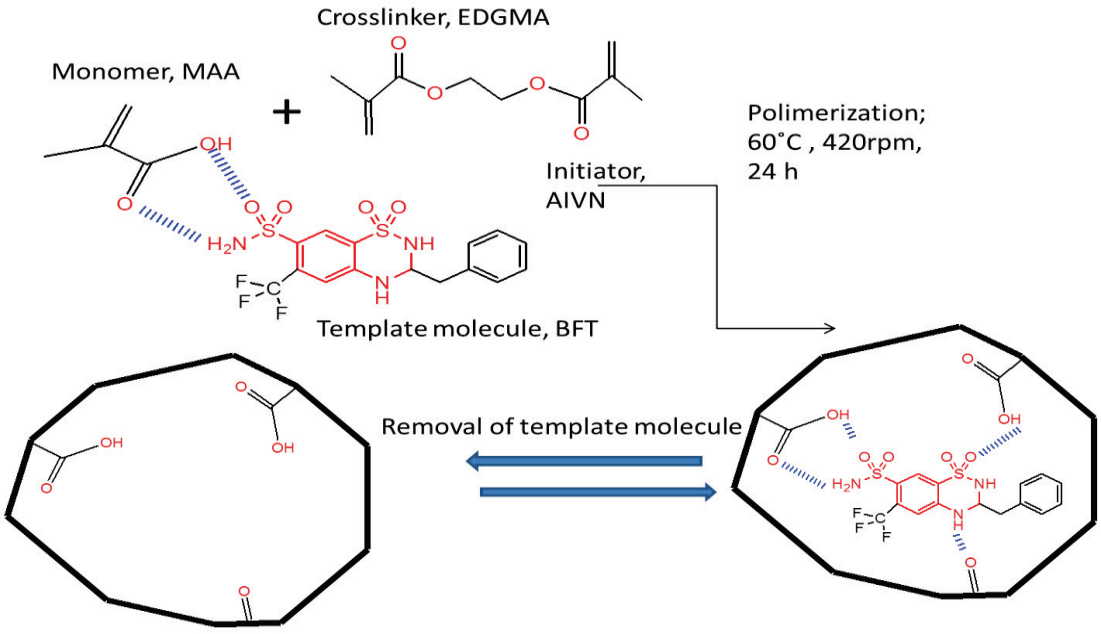

Figure 2.4. Schematic representation of MIP synthesis and template removal.

Removal of template molecule was done by using vacuum filtration system and 0.2 µm sartolon polyamide membrane filter. In order to achieve complete removal of template from the sorbent; it was swept and washed with methanol:acetic acid (90:10, v/v) mixture 10 times.

2.5.2. Synthesis of Silica Based MIIP&NIIP

In the inorganic part of imprinted material synthesis study, the molecularly imprinted inorganic polymer (MIIP) and its blind (NIIP) were synthesized by using 3-aminopropyltriethoxysilane (3-APTES), triethoxyphenylsilane (TEPS) as monomer, BFT as template molecule and tetraethoxysilane (TEOS) as crosslinker (Figure 2.5).

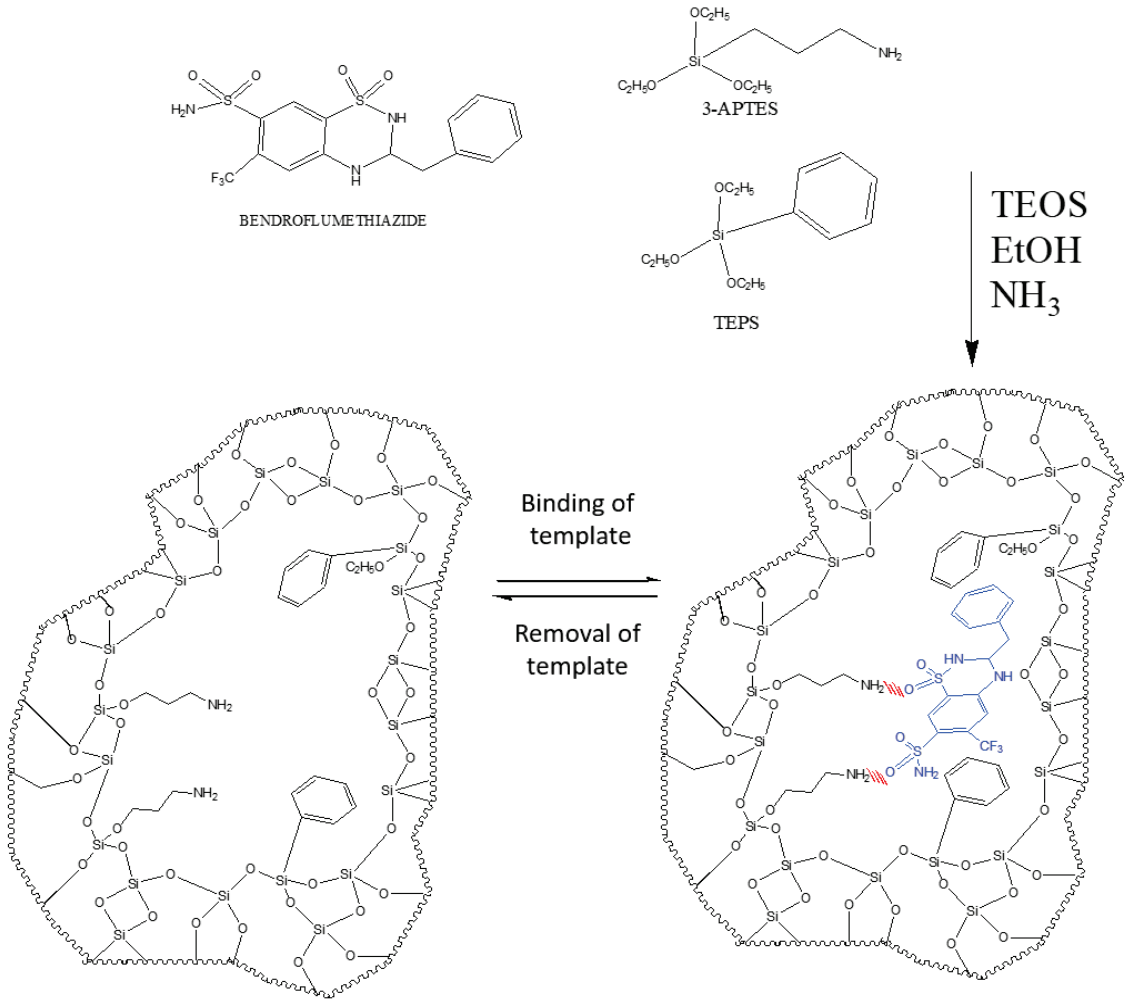

Figure 2.5. Schematic representation of MIIP synthesis and template removal

In order to obtain BFT imprinted silica, 1.0 mmol of template molecule was dissolved in 60.0 mL THF and 10.0 mL deionized water mixture. After 30 min stirring of mixture (450 rpm), 4.0 mmol APTES and 4.0 mmol TEPS were added to enable H-bonding with template molecule for 30 min. Then 16.0 mmol TEOS was added to solution and after 30 min, 10.0 mL of EtOH, 7.0 mL of $NH_3.H_2O$ were also added to complete the reaction in 24 hours. Because of the size of the resulting particles (nanometer scale), centrifugation was applied (1800 rpm, 15 min) to separate the solid phase and the particles were dried in oven at 60˚C for 24 hours. The template was removed by washing with 90:10 MeOH: HOAc (v/v) solution and centrifugation at 1800 rpm. This step was repeated 10 times for complete removal of the template. Finally, the obtained MIIP sorbent was dried at 60 ºC for 24 hours. All of the steps of this procedure were applied for non-imprinted inorganic polymer (NIIP) synthesis route, except addition of template molecule (BFT).

2.5.3. Characterization of Sythesized Sorbents

Images of MIP-NIPs, MIIP-NIIPs and filled capillaries were taken with scanning electron microscopy (SEM) to realizing the morphologies of synthesized materials and prove the filling of capillary.

Firstly, the selectivity of the synthesized materials to diuretic drug agents was tested as solid phase extraction (SPE) sorbent prior to CE. Further capillary filling experiments were continued with materials that give satisfactory results in sorption performance.

Also, elemental analysis was done for the determination of carbon, nitrogen contents in molecularly imprinted sorbents, before and after sorption of BFT.

2.5.3.1. Binding Characteristic Assay

Sample solutions were prepared as in Table 2.6. Sorbents (MIP, NIP, MIIP and NIIP) were respectively put into 10.0 mL of these solutions and shaken at 480 rpm for 24 hours. After that, the mixture was filtered through filter tip cellulose acetate or polyamide

membranes (0.2 μm pore size) to separate sorbents from solutions. Effluents were analyzed with CE-DAD by using 10.0 mM borate buffer (pH 9.4).

Table 2.6. Experimental parameters used in binding characteristic assay.

Standard concentrations of BFT	0.5, 1.0, 5.0, 10.0, 25.0, 50.0, 100.0 mgL^{-1}
Amount of sorbent	10.0 mg
Sample solution volume	10.0 mL
Sorption time	24 hour
Shaking speed	480 rpm
Ambient temperature	25.0˚C

2.5.3.2. Cross Sensitivity

100.0 mgL^{-1} mixtures of bendroflumethiazide, hydrochlorothiazide and chlorothiazide were prepared. 10.0 mL portions of mixture were respectively put into sorbents (MIP, NIP, MIIP and NIIP) and shaken with orbital shaker (at 480 rpm) for 24 hours. After that, the mixture was filtered through filter tip cellulose acetate or polyamide membranes (0.2 μm pore size) to separate sorbents from solutions. Effluents were analyzed with CE-DAD by using 10.0 mM borate buffer (pH 9.4). The sorption parameters are given in Table 2.7.

Table 2.7. Experimental parameters used in binding cross sensitivity study.

Standard concentration of BFT, HCT, CT mixture	100.0 mgL^{-1}
Amount of sorbent	10.0 mg
Sample solution volume	10.0 mL
Sorption time	24 hour
Shaking speed	480 rpm
Ambient temperature	25.0˚C

2.6. Preparation of Capillary Columns

This section of study is highly dependent on sorption properties of synthesized materials. In order to make appropriate comparison between them, sorbents were divided into two categories; silicate and functionalized silicate (Part I), molecularly imprinted ones (Part II).

Part I. includes amine modified, phenyl modified, amine-phenyl modified and unmodified silicates (Table 2.8). Hot synthesis procedure was converted to cold one by following another procedure (Wu et al. 2006) to make it applicable for capillary filling. Silica nanoparticles were synthesized as in functionalized mode (with necessary rearrangements) without further modification steps. There was no need to heat or refluxing system as in the hot synthesis and it is called as cold synthesis throughout the study.

In this procedure 2.79 mL TEOS and 22.2 mL EtOH were added to alkoxide solution that includes 0.638 mL $NH_3.H_2O$, 6.8 mL deionized water and 17.6 mL EtOH. After 3.5 hours stirring at room temperature, $4.79x10^{-4}$ mol TPES or APTES was added depending on purpose.

Sol-gel procedure was arranged in a way that reactants amount and 165.0 mL EtOH, 3.0 mL TEOS, 21 mL deionized water and 3.15 mL $NH_3.H_2O$ was used.

Table 2.8. Part I: Novel column synthesis with silicate and functionalized silicate.

Part I				
Identity	Procedure	Reaction starts	Filling mode	Layer
S1	Sol-gel	in column	with CE	x
S2	Cold synthesis (without APTES & PTES)	in column	with CE	x
S3	Cold synthesis (without APTES & PTES)	out of column	with CE	x
S4	Cold synthesis (without APTES & PTES)	in column	with CE	3
S5	Cold synthesis (without APTES & PTES)	in column	with CE	5

Part II. includes MIP-NIP and MIIP-NIIP sorbents (Table 2.9). Because the capillary wall consists of silica, binding MIIP or NIIP was provided by activating silica surface. The condensation reaction takes places between surface and sorbent. However, binding a polymeric molecule requires a coupling molecule that has both polymer and silicate ends. For this purpose, 3-(trimethoxysilyl) propyl methacrylate (98%, TMSPMA) was used prior to filling column with MIP or NIP. After conditioning the bare silica capillary, solution of 4.0 μL of TMSPMA in 1.0 mL of 0.006M HOAc was flushed in and the solution was kept in the capillary for 1.5 hours. Since the in-column results (NIPs and NIIPs) were not satisfactory, further MIP and MIIP fillings were done out of column.

Table 2.9. Part II: Novel column synthesis with MIP-NIP and MIIP-NIIP

Part II				
Identity	Procedure	Reaction starts	Filling mode	Layer
NIIP1	Silica Based NIIP	in column	with CE	x
NIP1	Polymer base NIP	in column	with CE	x
NIP1.1	Polymer base NIP	in column	with CE	1
NIP1.1.1	Polymer base NIP	in column	with CE	2
MIP2	Polymer base MIP	out of column	with shyringe	x
NIP2	Polymer base NIP	out of column	with shyringe	x
MIP3	Polymer Based MIP	out of column	with CE	3
NIP3	Polymer Based NIP	out of column	with CE	3
NIP3.1	Polymer Based NIP	out of column	with CE	5

CHAPTER 3

RESULTS AND DISCUSSION

3.1. Optimization of Instrumental Parameters

Optimization study for HPLC was done by changing the mobile phase composition and flow rate. Instrumental parameters were given in Table 2.1 and chromatograms were given in Figure 3.1.

Firstly, C18 column was used as the stationary phase and 80:20 methanol: water (acetic acid, pH 3.0) was used as the mobile phase to observe the chromatographic separation of bendroflumethiazide (BFT), hydrochlorothiazide (HCT) and chlorothiazide (CT). But chromatogram of BFT shows undesirable shouldered peak. Also, chromatograms of HCT and CT were similar to each other and broadened. To solve this problem mobile phase was changed to 80:20 methanol: water (phosphate buffer, pH 6.0).

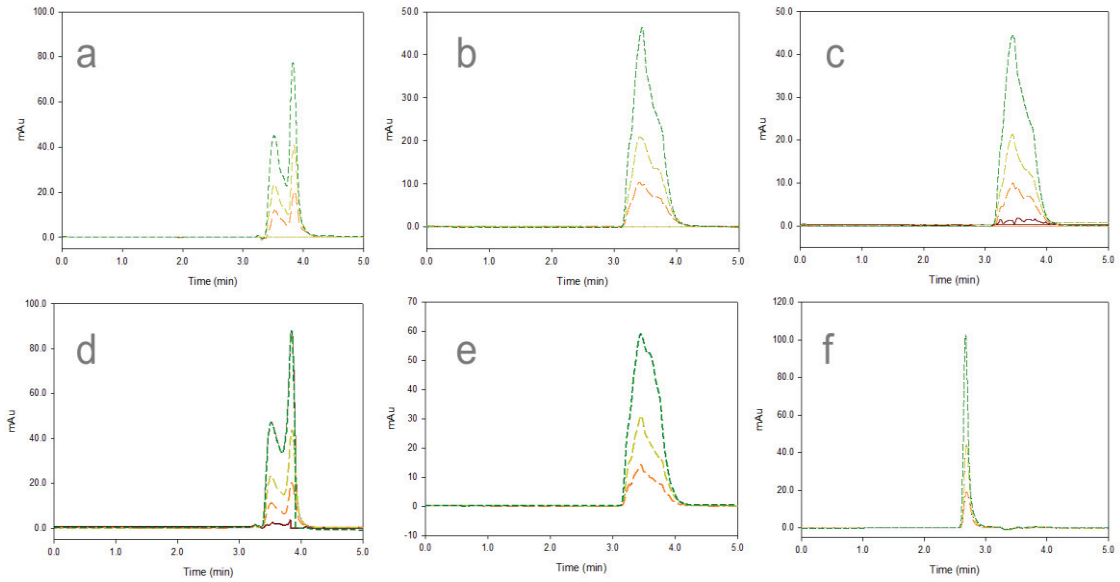

Figure 3.1. Chromatogram of BFT (a,d), HCT (b,e) and CT (c,f) (Agilent 1200 Series HPLC-DAD system, Supelco C18 (Lichrosphere RP 18-5, 25cm×4.6mm) column, 80:20 methanol: water (acetic acid, pH 3.0) mobile phase (a, b, c), 80:20 methanol: water (phosphate buffer, pH 6.0) mobile phase (d, e, f), 0.8 mL min^{-1} flow rate)

Bendroflumethiazide and hydrochlorothiazide peaks remained nearly the same. The most significant difference between the two mobile phases was seen in the chlorothiazide measurement. It gave a quite sharp and chromatographically more acceptable peak. Flow rate changes also did not give good results. No improvement was observed and therefore, calibration plots could not be prepared.

Within the scope of CE studies, for the selection of the appropriate buffer solution which is the most important variable; buffer concentration, buffer type, working parameters have been systematically changed and optimal conditions have been determined for the analysis of selected diuretics. Instrumental parameters were given in Table 2.2.

Hydrochlorothiazide, bendroflumethiazide and chlorothiazide solutions were prepared as 20.0 mg L^{-1}. Borate buffer (25.0 mM) was used as a background electrolyte that is suitable for initial trial for the separation of anionic substances. Analytes were given to the CE system first separately and then as a mixture. According to the electropherogram of analytes; chlorothiazide (pKa 6.85) has the highest, bendroflumethiazide (pKa 8.5) has the lowest retention time. Enough separation between HCT (pKa 7.9) and BFT (pKa 8.5) peak was not achieved because the pKa values are very close to each other (Figure 3.2. (a)). New electropherograms were obtained by changing the applied voltage, injection pressure, injection time, peak width, cassette temperature. But none of them gave satisfactory results. When background electrolyte was changed to phosphate buffer (pH 7.0) resolution was decreased. So, background electrolyte was fixed as the borate buffer and concentration was decreased to 10.0 mM. Resulting electropherogram shows better separation in terms of BFT and HCT peaks (Figure 3.2. (b)).

The buffer concentration highly affects the electroosmotic flow rate by changing the thickness of the diffuse double layer. So, reducing the appropriate buffer concentration shortens the peak migration times and increases the separation efficiency.

As a concluding remark, optimum parameters were set as; 25 kV voltage (with 6.0 W, 300 μA), 10.0 mM borate buffer (pH 9.4), 50.0 mbar injection for 10.0 sec, 30.0 ˚C cassette temperature, 2.5 Hz peak width. Calibration graphs of analytes is shown in Fig. 3.3. Limit of detection (LOD) values were calculated as 0.20 mg L^{-1}, 0.13 mg L^{-1}, 0.30 mg L^{-1} and limit of quantification (LOQ) was found as 0.69 mg L^{-1}, 0.44 mg L^{-1}, 0.99 mg L^{-1} for BFT, HCT and CT, respectively.

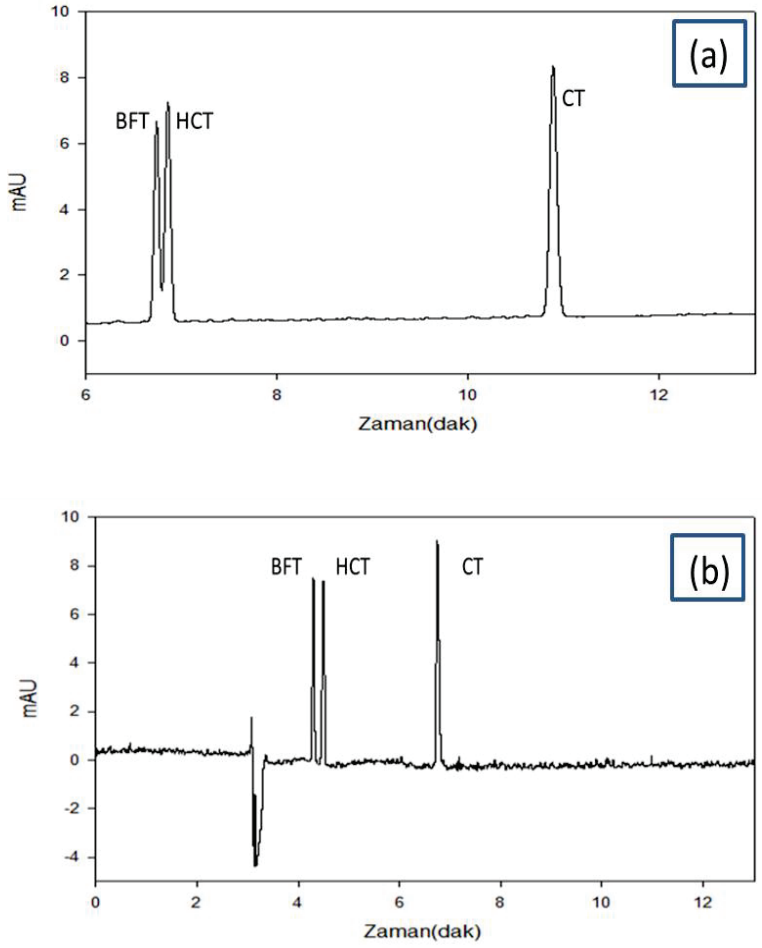

Figure 3.2. Electropherogram of analytes in (a) 25.0 mM borate buffer (b) 10.0 mM borate buffer.

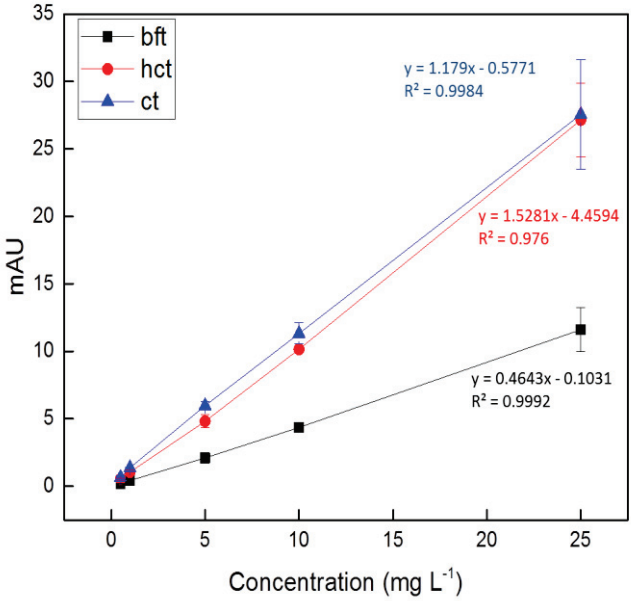

Figure 3.3. Calibration plot for bendroflumethiazide, hydrochlorothiazide and chlorothiazide.

3.2. Sorbents Prepared by Sol-Gel Method

3.2.1. Synthesis of Silica Sol-Gel

Particle size of the silica synthesized by sol gel routes was adjusted by differentiating the amount of TEOS and EtOH in the method as described in Section 2.4.1. Scanning electron microscope (SEM) image for 1. trial in Table 2.3. is shown in Figure 3.4.

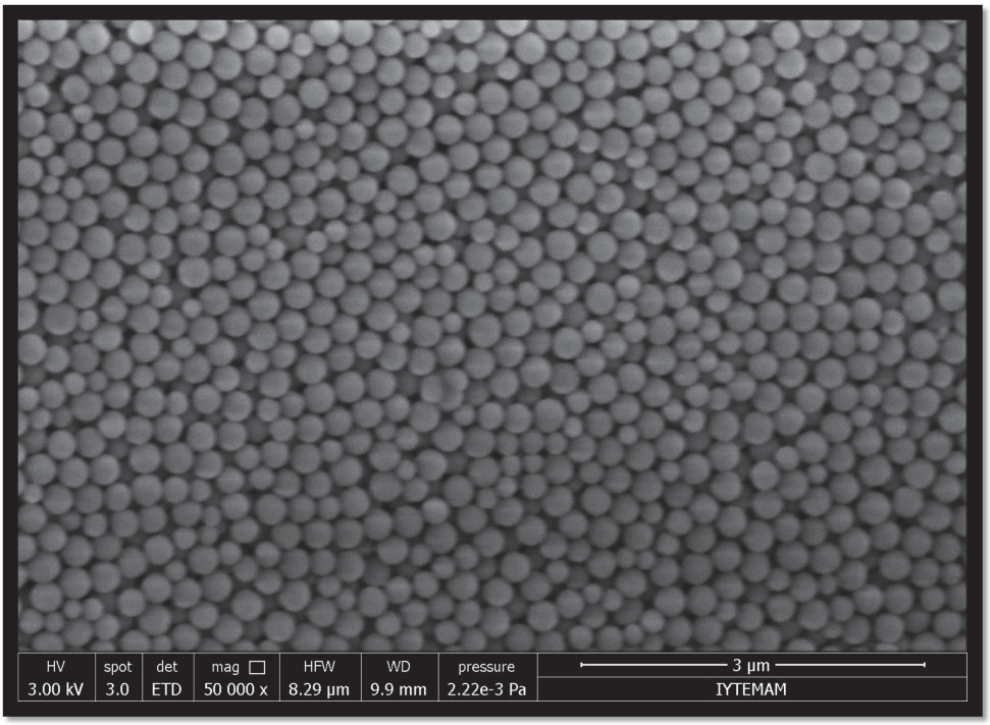

Figure 3.4. SEM image of silica sol-gel.

Changing the amount of TEOS did not cause a significant change in particle size which was between 120-350 nm. However, there was a change in the amount of silica gel produced.

In the second part, while the other parameters were kept constant, the amount of ethanol was changed (parameters were given in Table 2.3). Increasing the solvent amount would cause decreasing the particle size (Figure 3.5). The reason was the increment in the space among the particles. During the formation of the sol gel, reduced possibility of agglomeration of the particles resulted with the particle stayed in the nanosize instead of growing together.

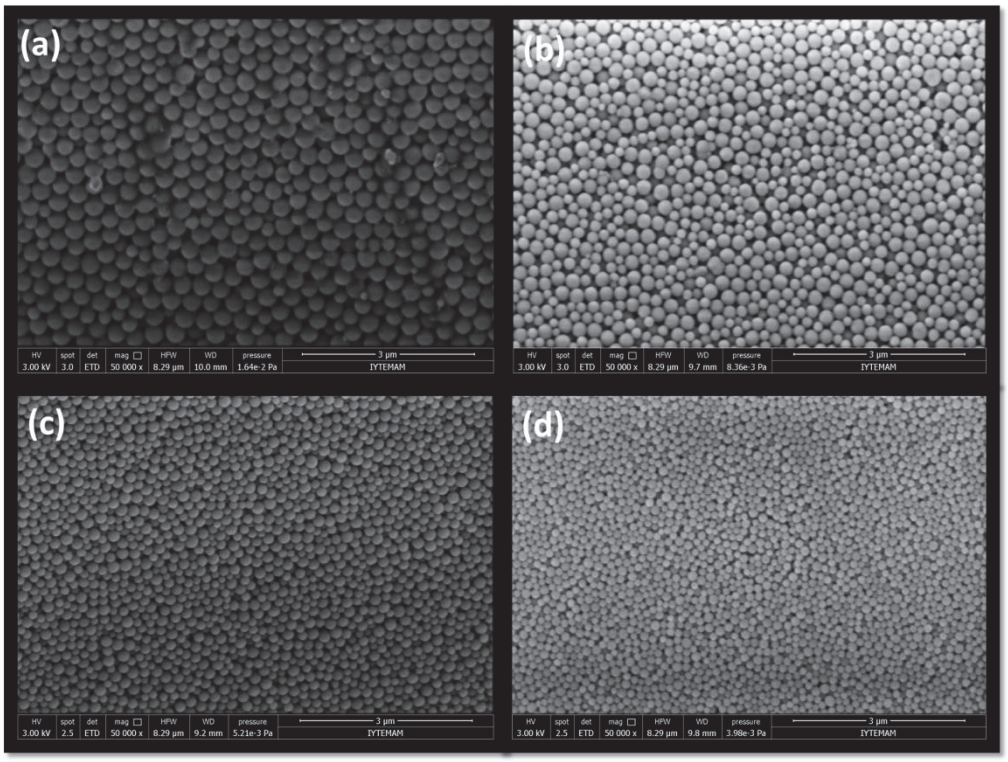

Figure 3.5. SEM images of silica gel when (a) 15 mL EtOH, (b) 25 mL EtOH, (c) 45 mL EtOH, (d) 55 mL EtOH were used in the synthesis procedure.

3.2.2. Surface Modification of Silicate

The detailed high-resolution images of the sample morphology and elemental identification (with relative quantitative compositions) of amine functional groups on surface of silicate structures were established by using SEM/EDX (Figure 3.6 and Figure 3.7).

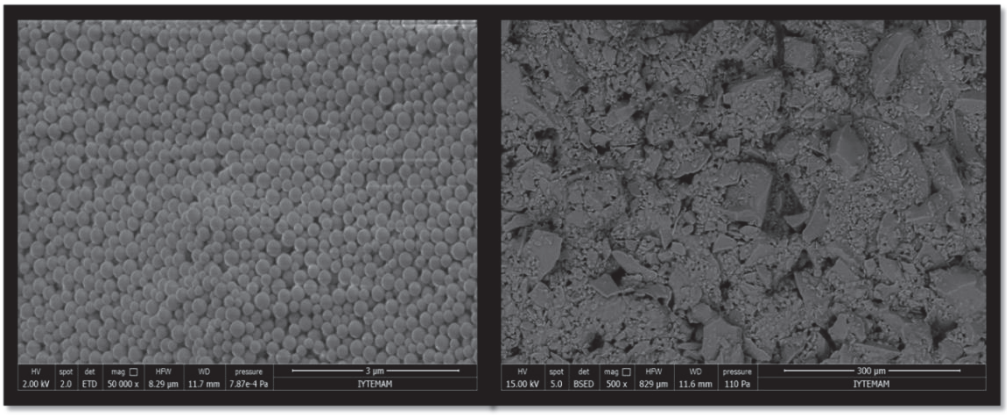

Figure 3.6. SEM images of silicate with amine functional group.

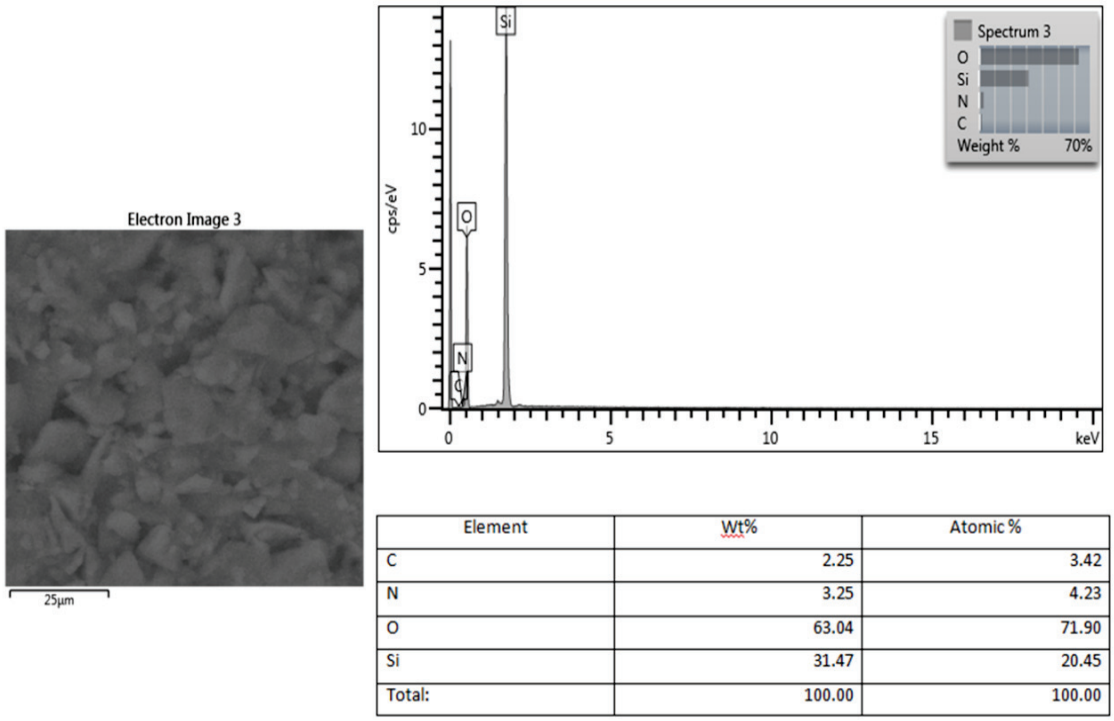

Element	Wt%	Atomic %
C	2.25	3.42
N	3.25	4.23
O	63.04	71.90
Si	31.47	20.45
Total:	100.00	100.00

Figure 3.7. EDX results of silicate with amine functional group.

3.2.3. Characterization of Sythesized Sorbents

3.2.3.1. Sorption Performance of Synthesized Sorbents

Sorption capacities of amine-modified, phenyl-modified, both amine-phenyl-modified and unmodified silica sol-gel particles are shown in (Figure 3.8). The Q value shows the amount of analytes (mmol) which are retained on 1.0 g of the sorbent. Since no selective sorption is expected with these type of sorbents analytes were loaded as mixture.

According to the results, unmodified silica shows highest sorption capacity for all of the analytes. This must be due to the H-bonding and electrostatic attraction between the analyte molecules and silica surfaces. It is expected that sorption of analytes will be increased by H-bonding with amine groups or π-π stacking of phenyl groups. However, there is no such an effect. This can be indication of the sorption profiles of amine or phenyl modified sorbents do not show an expected trend.

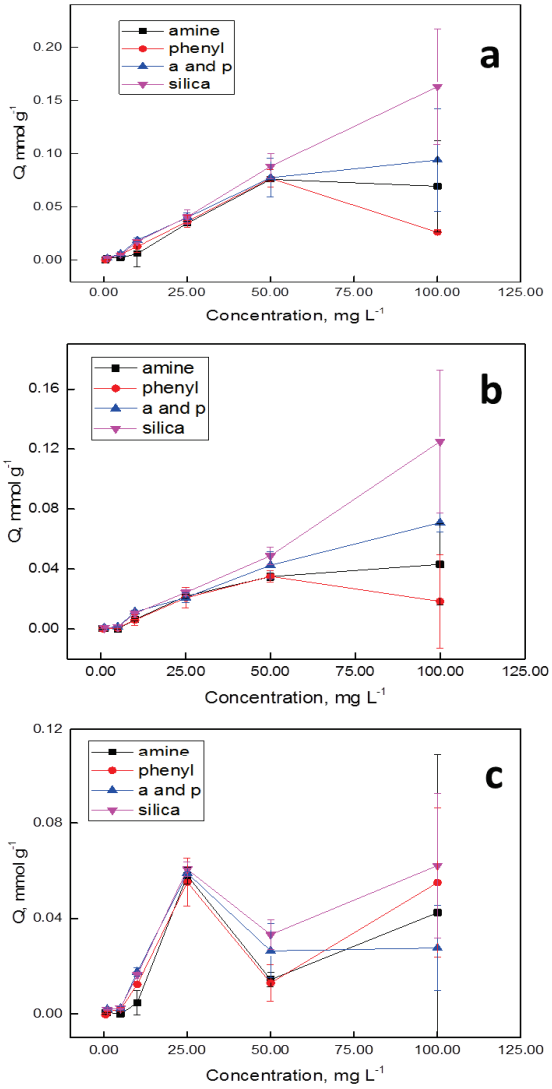

Figure 3.8. Sorption capacities of amine-modified, phenyl-modified, both amine-phenyl-modified and unmodified silica sol-gel particles for (a) BFT, (b) HCT, (c) CT.

3.3. Molecularly Imprinted Technology Based Sorbents

3.3.1. Synthesis of MIP and NIP

Structural morphologies of MIPs and NIPs were investigated by SEM (Figure 3.9). As expected, no obvious differences between MIPs and NIPs were observed since any possible change would occur in molecular level.

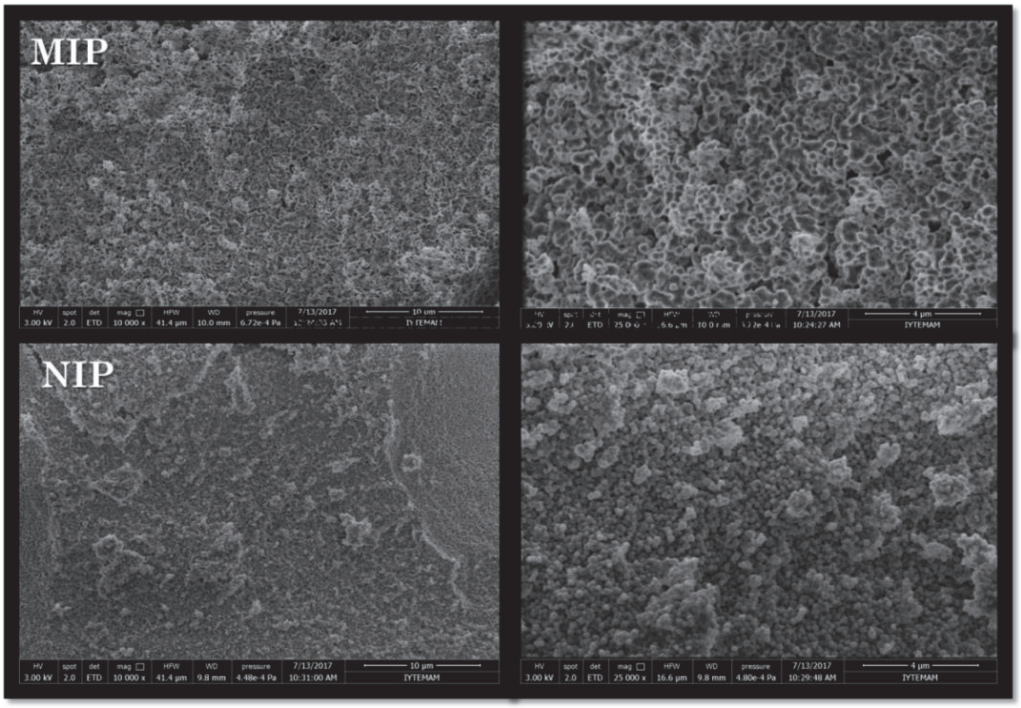

Figure 3.9. SEM images of MIP and NIP.

The template was removed from the synthesized polymers by washing with 90:10 MeOH: HOAc (v/v) solution. After 10 wash (as mentioned in Section 2.5.1), the BFT was completely removed from the polymer. The electropherogram of BFT before and after template removal from the sorbent is shown in Figure 3.10.

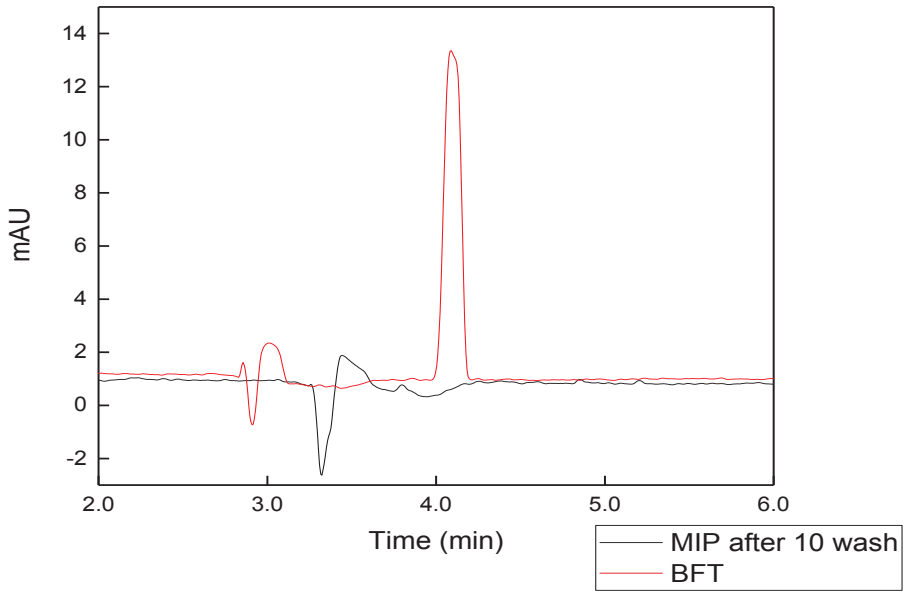

Figure 3.10. The electropherogram of BFT before and after template removal from the MIP sorbent.

3.3.2. Synthesis of Silica Based MIIP and NIIP

Structural properties of MIIPs and NIIPs were investigated by SEM (Figure 3.11). As expected, no obvious differences between MIIPs and NIIPs were observed. The template was removed from the synthesized silica-based polymers by washing with 90:10 MeOH: HOAc (v/v) solution. After 10 wash BFT was completely removed from the polymer. The electropherogram of before and after template removal is shown in Figure 3.12.

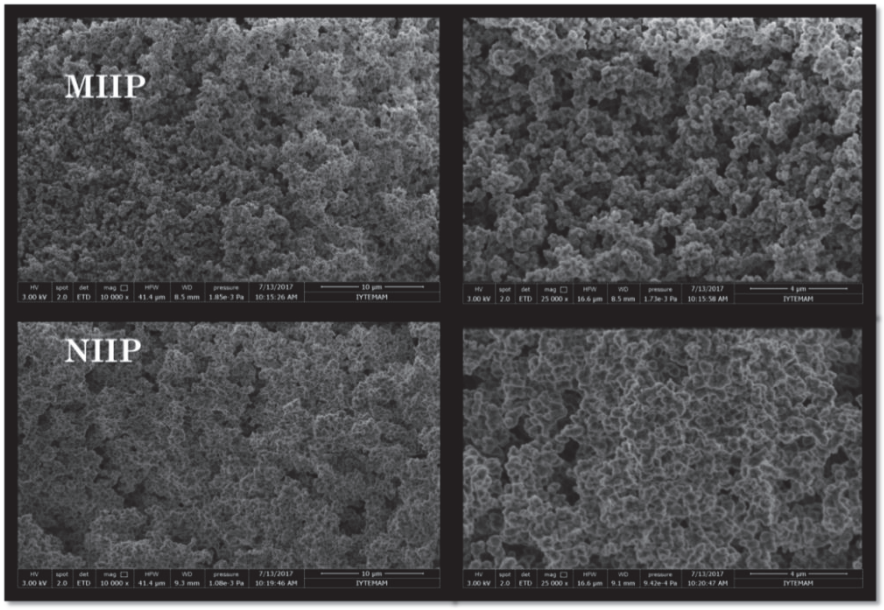

Figure 3.11. SEM images of MIIP and NIIP.

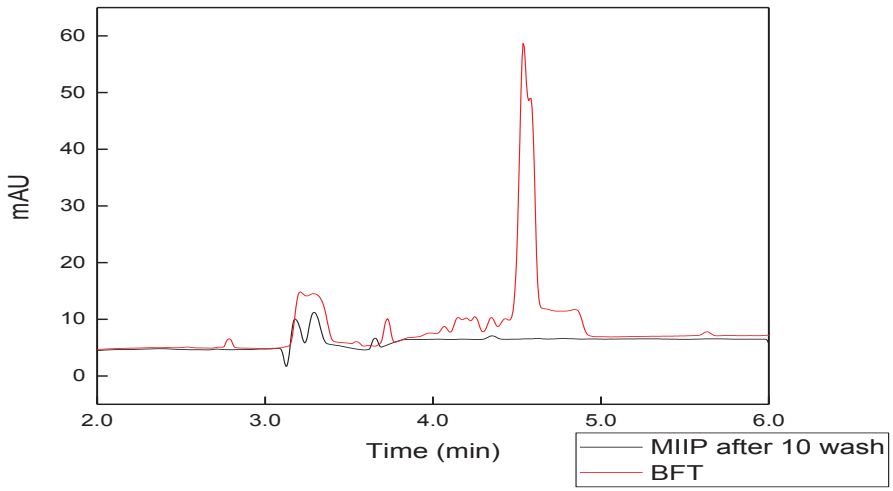

Figure 3.12. The electropherogram of BFT before and after template removal from the MIIP sorbent.

3.3.3. Characterization of Sythesized Sorbents

3.3.3.1. Binding Characteristic Assay

Sorption capacities of MIP and NIP particles are given in Figure 3.13. The Q value shows the amount of analytes (mmol) which are retained on 1.0 g of the MIP or NIP sorbent. Around 50.0 mg L^{-1}, the difference between sorption capacities of MIP and NIP is become obvious. Almost linear increase in the sorption capacity of MIP is an indication of selectivity of the sorbent to BFT.

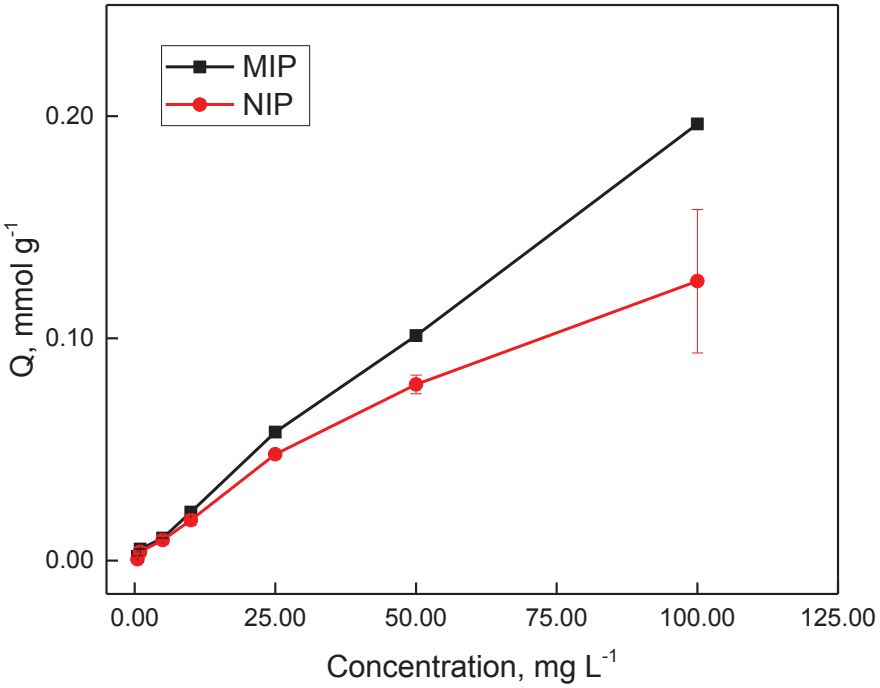

Figure 3.13. Sorption capacities of MIP and NIP.

In similar manner, the sorption properties of MIIP and NIIP particles were examined. Their sorption capacities are given in Figure 3.14. The difference between sorption capacities of MIIP and NIIP is not conclusive. Unlike the profiles in the sorption of molecularly imprinted polymers, sorption profiles of MIIP and NIIP do not show an expected trend and are irreproducible. This result makes MIIP and NIP unreliable for specific sorption of BFT.

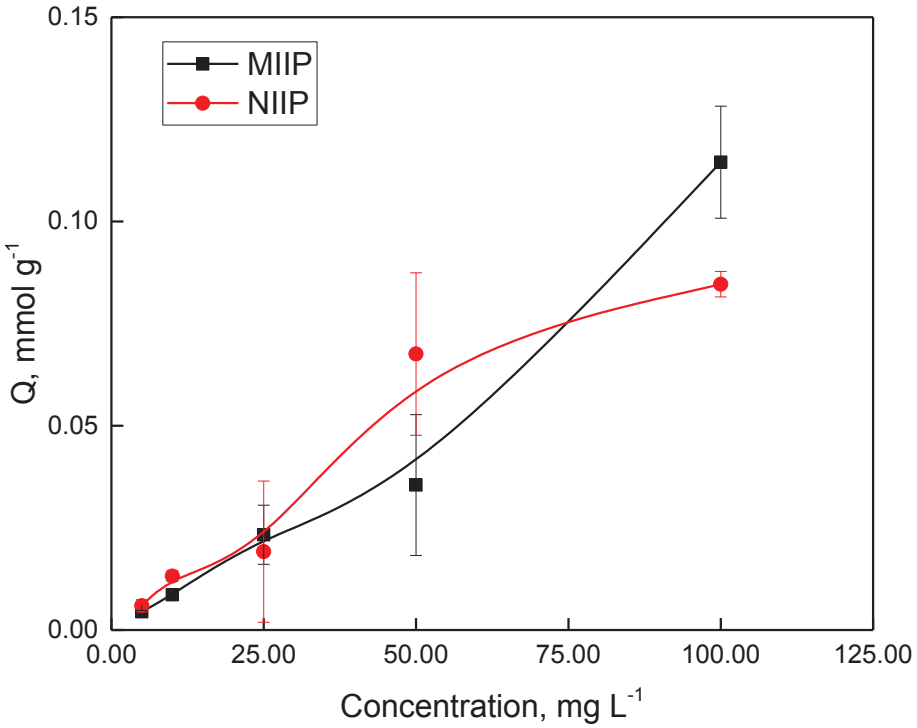

Figure 3.14. Sorption capacities of MIIP and NIIP

3.3.3.2. Cross Sensitivity

Figure 3.15. illustrates the sorption capacities of MIP and NIP to structurally related compounds. The procedure was explained in Section 2.5.3.2.

In presence of HCT and CT, which are structurally related compounds with BFT, MIP shows better sorption capacity towards the bendroflumethiazide than NIP. This is the evidence of the successfully generated analyte (BFT) cavities in MIP. For HCT and CT, both of the MIP and NIP, show nearly the same sorption. Also, Q values for these two compounds are comparatively lower than that of BFT.

The sorption capacities of MIIP and NIIP to BFT in presence of HCT and CT is given in Figure 3.16. The procedure was explained in Section 2.5.3.2. There is no obvious difference between MIIP and NIIP sorption capacities for any compound. This can be indication of the sorption which occurs mainly on the surface of the sorbents (both MIIP and NIIP) rather than the specific cavities created throughout the solid sorbent.

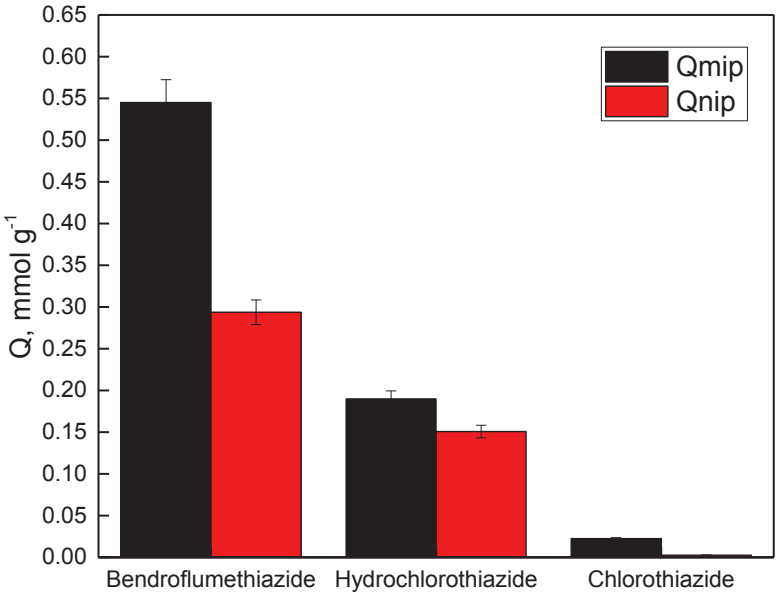

Figure 3.15. Sorption capacity of MIP and NIP in the presence of structurally related compounds.

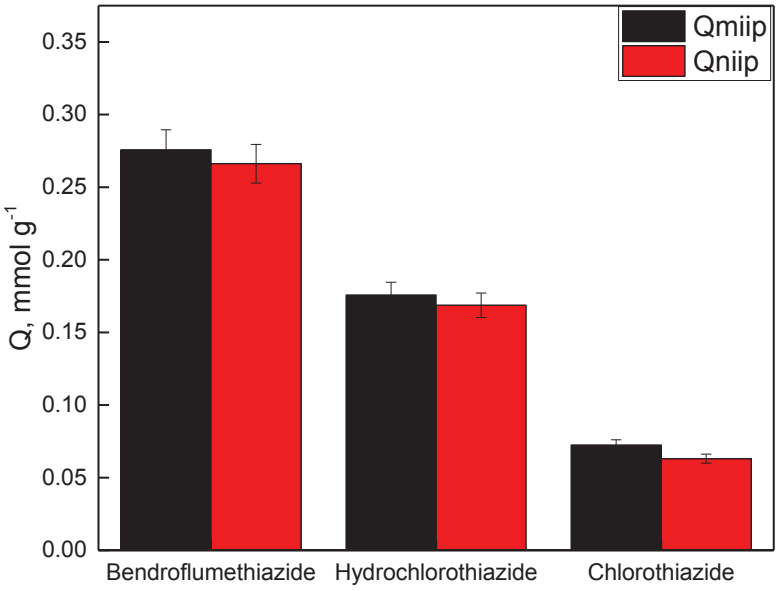

Figure 3.16. Sorption capacity of MIIP and NIIP in the presence of structurally related compounds.

3.4. Preparation of Capillary Columns

Scanning electron microscope (SEM) image of capillary column prepared as explained in Tables 2.8. and 2.9 is shown in Figures 3.17 and 3.18. Structural morphologies can be compared by the help of these images.

Figure 3.17 shows bare silica capillary that was not modified and considered as a blank material.

Figure 3.18 shows SEM image of S2 (unmodified silica) which was created by cold synthesis and the reaction took place in column. Filling of the solution into capillary was achieved by CE injection.

Figure 3.19 shows SEM image of MIP3 which was created by molecular imprinting method. The reaction started out of the column and was filled into column by using injection system of CE device.

Remaining column development studies (Table 2.8. and Table 2.9) did not give satisfactory results in the aspect of physical morphologies. Also, analysis was done with the usage of these prepared columns but no meaningful electrochromatogram was obtained.

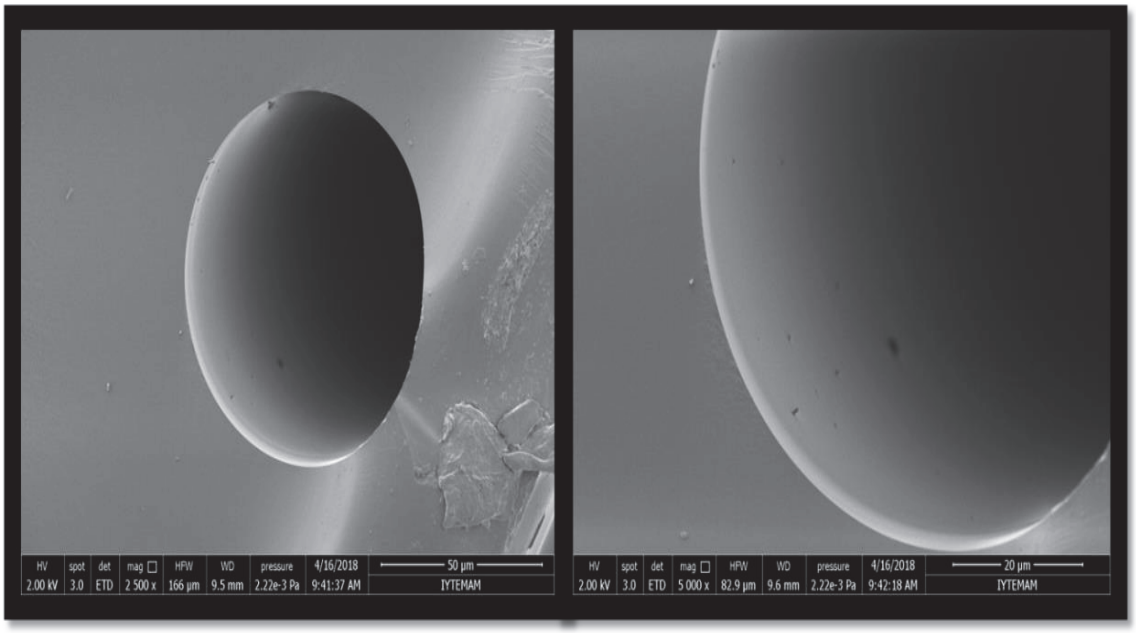

Figure 3.17. SEM image of bare silica capillary.

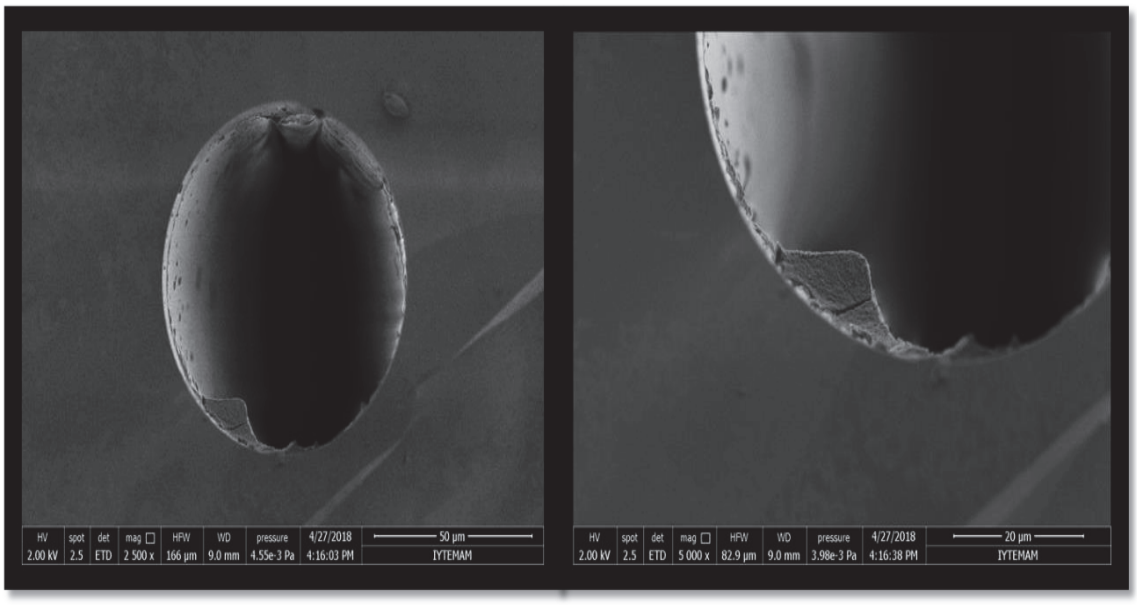

Figure 3.18. SEM image of silica capillary that was filled with unmodified silica sorbent.

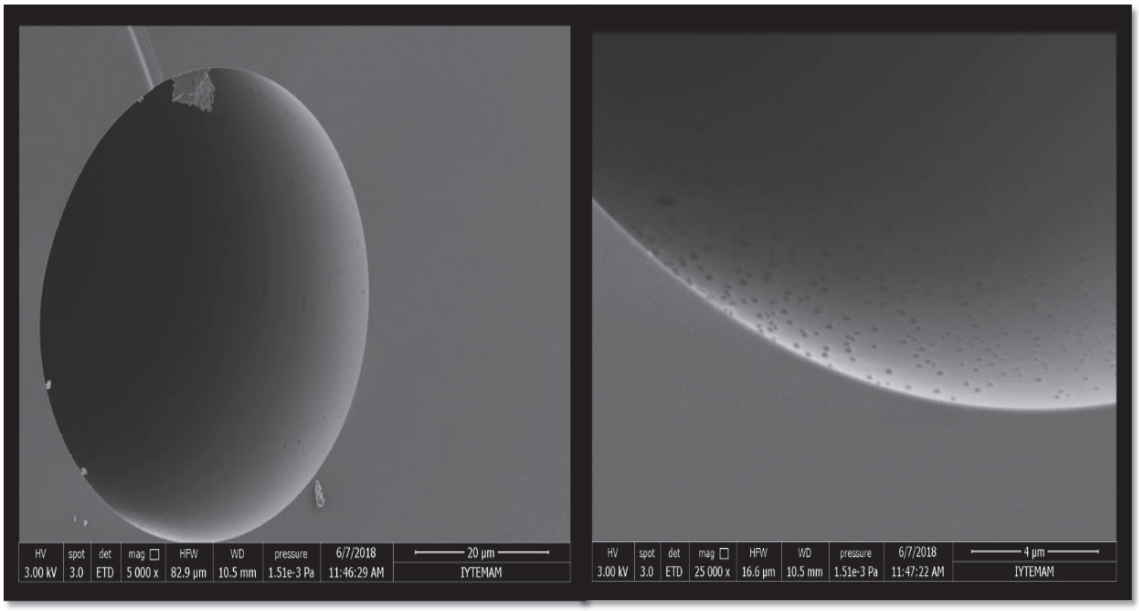

Figure 3.19. SEM image of silica capillary that was filled with MIP sorbent.

CHAPTER 4

CONCLUSION

In the route of novel column development for CEC analysis, selection of the stationary phase is one the most important parts. For this purpose, possible sorbents that can be used as stationary phase in the column was investigated prior to CE-DAD analysis.

Firstly, the optimum parameters for CE analysis were determined as; 25 kV voltage (with 6.0 W, 300 μA), 10.0 mM borate buffer (pH 9.4), 50.0 mbar injection for 10.0 sec, 30.0 ˚C cassette temperature. Calibration graphs of BFT, HCT and CT were obtained under these optimum conditions. Limit of detection (LOD) and limit of quantification (LOQ) values were calculated as between 0.20 mg L^{-1} ~ 0.30 mg L^{-1} and 0.44 mg L^{-1} ~ 0.99 mg L^{-1}, respectively. Then, sorption studies were carried out. Two different methodologies, sol-gel and molecularly imprinting methodology were used for synthesis of sorbents and compared in terms of sorption capacities.

Synthesis of silicate structures was carried out using the sol-gel route with slight modifications of the one-step Stöber process. Also, silica surface was functionalized with 3-APTES and TEPS to make H-bonding and π-π stacking. According to the results, unmodified silica has shown the highest sorption capacity for all analytes (BFT, HCT, CT). So it was chosen as stationary phase of capillary column, between sol-gel group.

Molecular imprinting polymers were prepared by using organic and inorganic precursors, called MIP and MIIP, respectively. The sorption capacity (Q value) and selectivity of imprinted polymers were investigated. They were synthesized for the specific recognition of BFT prior to the determination by CE-DAD, because it was the largest molecule among the analytes. MIP has shown quantitative sorption when compared with its blank (NIP) and MIIP. Also, it was proven that MIP can be used for selective determination of BFT.

In CEC-DAD analysis, results were not satisfactory and reproducible. Noisy background complicate the electropherogram and it was not possible to identify if there is a peak or not. It should be fixed and column development can be regenerated. For the future studies, coupling the CE with MS will be the best solution fort he enhancement in sensitivity.

REFERENCES

AgilentTechnologies. 2014. "High Performance Capillary Electrophoresis." Agilent Technologies,accessed13May2018.https://www.agilent.com/cs/library/primers/pdf.

Alnajjar, A. O., A. M. Idris, M. V. Attimarad, A. M. Aldughaish, and R. E. Elgorashe. 2013. "Capillary electrophoresis assay method for metoprolol and hydrochlorothiazide in their combined dosage form with multivariate optimization." *J Chromatogr Sci* 51 (1):92-7. doi: 10.1093/chromsci/bms107.

Botre, F. 2008. "New and old challenges of sports drug testing." *J Mass Spectrom* 43 (7):903-7. doi: 10.1002/jms.1455.

Boyaci, E., A. Cagir, T. Shahwan, and A. E. Eroglu. 2011. "Synthesis, characterization and application of a novel mercapto- and amine-bifunctionalized silica for speciation/sorption of inorganic arsenic prior to inductively coupled plasma mass spectrometric determination." *Talanta*85(3):1517-25.doi:10.1016/j.talanta. 2011. 06.021.

Cadwallader, A. B., X. de la Torre, A. Tieri, and F. Botre. 2010. "The abuse of diuretics as performance-enhancing drugs and masking agents in sport doping: pharmacology, toxicology and analysis." *Br J Pharmacol* 161 (1):1-16. doi: 10.1111/j.1476-5381.2010.00789.x.

Cheong, W. J., F. Ali, Y. S. Kim, and J. W. Lee. 2013. "Comprehensive overview of recent preparation and application trends of various open tubular capillary columns in separation science." *JChromatogrA* 1308:1-24.doi:10.1016/ j.chroma.2013.07.107.

Chun Deng, Yaping Zhong, Yu He, Yili Ge, Gongwu Song. 2015. "Selective determination of trace bisphenol a using molecularly imprinted silica nanoparticles containing quenchable fluorescent silver nanoclusters." *Microchimica Acta* 183 (1):431-439. doi: 10.1007/s00604-015-1662-x.

D. Thieme, J. Grosse, R. Lang, R.K. Mueller, A. Wahl. 2001. "Screening, confirmation and quantitation of diuretics in urine for doping control analysis by high-performance liquid chromatography–atmospheric pressure ionisation tandem mass spectrometry." *Journal of Chromatography B: Biomedical Sciences and Applications* 757 (1):49-57. doi: 10.1016/s0378-4347(01)00058-5.

Danks, A. E., S. R. Hall, and Z. Schnepp. 2016. "The evolution of 'sol–gel' chemistry as a technique for materials synthesis."*Mater.Horiz.*3(2):91-112.doi:10.1039/c5 mh00260e.

Deventer, K., G. Baele, P. Van Eenoo, O. J. Pozo, and F. T. Delbeke. 2009. "Stability of selected chlorinated thiazide diuretics." *J Pharm Biomed Anal* 49 (2):519-24. doi: 10.1016/j.jpba.2008.11.001.

Deventer, K., O. J. Pozo, P. Van Eenoo, and F. T. Delbeke. 2009. "Detection of urinary markers for thiazide diuretics after oral administration of hydrochlorothiazide and altizide-relevance to doping control analysis." *J Chromatogr A* 1216 (12):2466-73. doi: 10.1016/j.chroma.2009.01.032.

Eeltink,S. and W.T.Kok. 2006. "Recent applications in capillary electrochromatography." *Electrophoresis*27(1):84-96.doi:10.1002/elps.2005005 52.

Eeltink, S., G. P. Rozing, and W. T. Kok. 2003. "Recent applications in capillary electrochromatography."*Electrophoresis*24(22-23):3935-61.doi:10.1002/elps.20 0305638.

Giron, A. J., K. Deventer, K. Roels, and P. Van Eenoo. 2012. "Development and validation of an open screening method for diuretics, stimulants and selected compounds in human urine by UHPLC-HRMS for doping control." *Anal Chim Acta* 721:137-46. doi: 10.1016/j.aca.2012.02.002.

Goebel, Catrin, Graham J. Trout, and Rymantas Kazlauskas. 2004. "Rapid screening method for diuretics in doping control using automated solid phase extraction and liquid chromatography-electrospray tandem mass spectrometry." *Analytica Chimica Acta* 502 (1):65-74. doi: 10.1016/j.aca.2003.09.062.

Huang, Y. P., Z. S. Liu, C. Zheng, and R. Y. Gao. 2009. "Recent developments of molecularly imprinted polymer in CEC." *Electrophoresis* 30 (1):155-62. doi: 10.1002/elps.200800410.

Iacob, B. C., E. Bodoki, and R. Oprean. 2014. "Recent advances in capillary electrochromatography using molecularly imprinted polymers." *Electrophoresis* 35 (19):2722-32. doi: 10.1002/elps.201400253.

J. Barbosa , D. Barron , J.L. Beltran , S. Butı. 1998. "On the role of solvent in acid–base equilibria of diuretics in acetonitrile–water mixed solvents." *Talanta* 45 (5):817-827. doi: 10.1016/s0039-9140(97)00167-7.

Jiskra, Jan. 2002. *Capillary Electrochromatography Fundamentals and Applications*: Eindhoven : Technische Universiteit Eindhoven.

Juan Tamargo, Julian Segura, Luis M Ruilope. 2014. "Diuretics in the treatment of hypertension. Part 1: thiazide and thiazide-like diuretics." *Expert Opinion on Pharmacotherapy* 15 (4):527-47. doi: 10.1517/14656566.2014.879118.

Junjie, L., Y. Mei, H. Danqun, H. Changjun, L. Xianliang, W. Guomin, and F. Dan. 2013. "Molecularly imprinted polymers on the surface of silica microspheres via sol-gel method for the selective extraction of streptomycin in aqueous samples." *J Sep Sci* 36 (6):1142-8. doi: 10.1002/jssc.201200869.

K.D. Bartle, R.A. Carney, A. Cavazza, M.G. Cikalo, P. Myers, M.M. Robson, S.C.P. Roulin, K. Sealey. 2000. "Capillary electrochromatography on silica columns: factors influencing performance." *Journal of Chromatography A* 892:279–290.

doi: S0021-9673(00)00150-3.

Kasicka, V. 2012. "Recent developments in CE and CEC of peptides (2009-2011)." *Electrophoresis* 33 (1):48-73. doi: 10.1002/elps.201100419.

Kitagawa, F., and K. Otsuka. 2011. "Recent progress in capillary electrophoretic analysis of amino acid enantiomers." *J Chromatogr B Analyt Technol Biomed Life Sci* 879 (29):3078-95. doi: 10.1016/j.jchromb.2011.03.016.

Ku Fu Hsu, Kuei-Yu Chien, Guo Ping Chang-Chien, Su Fan Lin, Pei Hsuan Hsu and Mei-Chich Hsu. 2011. "Liquid Chromatography-Tandem Mass Spectrometry Screening Method for the Simultaneous Detection of Stimulants and Diuretics in Urine."*Journal of Analytical Toxicology* 35 (9):665-674. doi: 10.1093 /anatox/ 35.9.665.

Larry L. Hench, Jon K. West. 1990. "The sol-gel process." *Chemical Reviews* 90 (1):33-72. doi: 10.1021/cr00099a003.

Lemke, T.L. and D.A. Williams.2012. *Foye's Principles of Medicinal Chemistry*: Lippincott Williams & Wilkins.

Loffing,J. 2004. "Paradoxical antidiuretic effect of thiazides in diabetes insipidus: another piece in the puzzle."*JAmSocNephrol*15(11):2948-50.doi:10.1097/01.ASN.0000 146568.82353.04.

Luis, M. 2002. "Micellar electrokinetic capillary chromatography analysis of diuretics in pharmaceutical formulations."*Talanta*57(2):223-31.doi:10.1016/s0039-9140 (02) 00018-8.

Lv, Yun-Kai, Li-Min Wang, Shuai-Lei Yan, Xiao-Hu Wang, and Han-Wen Sun. 2012. "Synthesis and characterization of molecularly imprinted poly(methacrylic acid)/silica hybrid composite materials for selective recognition of lincomycin in aqueous media." *Journal of Applied Polymer Science* 126 (5):1631-1636. doi: 10.1002/app.36795.

M. Ganzera, I. Nischang. 2010. "The Use of Capillary Electrochromatography for Natural Product Analysis–Theoretical Background and Recent Applications."*Current Organic Chemistry* 14 (16):1769-1780. doi: 1385-2728/10.

Morra, V., P. Davit, P. Capra, M. Vincenti, A. Di Stilo, and F. Botre. 2006. "Fast gas chromatographic/mass spectrometric determination of diuretics and masking agents in human urine: Development and validation of a productive screening protocol for antidoping analysis."*JChromatogrA*1135(2):219-29.doi: 10.1016/ j.chroma.2006.09.034.

Mu, L. N., Z. H. Wei, and Z. S. Liu. 2015. "Current trends in the development of molecularly imprinted polymers in CEC." *Electrophoresis* 36 (5):764-72. doi: 10.1002/elps.201400389.

Olcer, Y. A., M. Demirkurt, M. M Demir, and A. E. Eroglu. 2017. "Development of

molecularly imprinted polymers (MIPs) as a solid phase extraction (SPE) sorbent for the determination of ibuprofen in water." *RSC Advances* 7 (50):31441-31447. doi: 10.1039/c7ra05254e.

Ou, J., Z. Liu, H. Wang, H. Lin, J. Dong, and H. Zou. 2015. "Recent development of hybrid organic-silica monolithic columns in CEC and capillary LC." *Electrophoresis* 36 (1):62-75. doi: 10.1002/elps.201400316.

Pena Crecente, R. M., C. G. Lovera, J. B. Garcia, C. H. Latorre, and S. G. Martin. 2016. "Ultrasound-assisted magnetic solid-phase extraction for the determination of some transition metals in Orujo spirit samples by capillary electrophoresis." *Food Chem* 190:263-9. doi: 10.1016/j.foodchem.2015.05.101.

Rosa Ventura , Jordi Segura. 1996. "Detection of diuretic agents in doping control." *Journal of Chromatography B: Biomedical Sciences and Applications* 687(1): 127-44. doi: 10.1016/s0378-4347(96)00279-4.

Rosa Ventura , Teresa Nadal, Pilar Alcalde, J.Antonio Pascual, and Jordi Segura. 1993. "Fast Screening Method for Diuretics, Probenecid and Other Compounds of Doping Interest." *Journal of Chromatography A* 655 (2):233-42. doi: 10.1016/ 0021-9673(93)83228-k.

Sarafraz-Yazdi, Ali, and Nourolhoda Razavi. 2015. "Application of molecularly-imprinted polymers in solid-phase microextraction techniques." *TrAC Trends in Analytical Chemistry* 73:81-90. doi: 10.1016/j.trac.2015.05.004.

Schappler, J., D. Guillarme, S. Rudaz, and J. L. Veuthey. 2008. "Microemulsion electrokinetic chromatography hyphenated to atmospheric pressure photoionization mass spectrometry." Electrophoresis 29 (1):11-9.(2)doi: 10.1002/ elps.200700647.

Schubert, U., and N. Hüsing. 2000. *Synthesis of Inorganic Materials*: Wiley.Sellergen, B. 2000. *Molecularly Imprinted Polymers: Man-Made Mimics of Antibodies and their Application in Analytical Chemistry*: Elsevier Science.

Siren, H., R. Shimmo, P. Sipola, S. Abenet, and M. L. Riekkola. 2008. "Capillary electrophoresis of diuretics and probenecid in methanol." *J Chromatogr A* 1198-1199:215-9. doi: 10.1016/j.chroma.2008.05.026.

Smith, Norman. 1999. *Capillary ElectroChromatography*. California: Beckman Coulter.

Strandwitz, Nicholas C., and Galen D. Stucky. 2009. "Hollow Microporous Cerium Oxide Spheres Templated By Colloidal Silica." *Chemistry of Materials* 21 (19):4577-4582. doi: 10.1021/cm901516b.

Tang, S., S. Liu, Y. Guo, X. Liu, and S. Jiang 2014. "Recent advances of ionic liquids and polymeric ionic liquids in capillary electrophoresis and capillary electrochromatography." JChromatogA1357:147-57. doi:10.1016/j.chroma.2014.

Tarongoy, F. M., Jr., P. R. Haddad, R. I. Boysen, M. T. Hearn, and J. P. Quirino. 2016. "Open tubular-capillary electrochromatography: Developments and applications

from 2013 to 2015." *Electrophoresis* 37 (1):66-85. doi: 10.1002/elps.201500339.

Tse-Tsung Ho, Zu-Guang Li, Hui-Yi Lin and Maw-Rong Lee. 2013. "Determination of Diuretics in Urine Using Immobilized Multi-Walled Carbon Nanotubes in Hollow Fiber Liquid-Phase Microextraction Combined with Liquid Chromatography-Tandem Mass Spectrometry." *Journal of the Chinese Chemical Society* 60 (8):1033-42. doi: 10.1002/jccs.201200603.

WADA. 2018a. "PROHIBITED LIST DOCUMENTS." accessed 11 May 2018. https://www.wada-ama.org/en/resources/science-medicine/prohibiteddocuments.

WADA. 2018b. "Technical Document – TD2018MRPL." accessed 11 May 2018. https://www.wada-ama.org/sites/default/files/resources/files/td2018finaleng.pdf.

Wu, M., R. Wu, Z. Zhang, and H. Zou. 2011. "Preparation and application of organic-silica hybrid monolithic capillary columns." *Electrophoresis* 32 (1):105-15. doi: 10.1002/elps.201000349.

Wu, Z., H. Xiang, T. Kim, M. S. Chun, and K. Lee. 2006. "Surface properties of submicrometer silica spheres modified with aminopropyltriethoxysilane and phenyltriethoxysilane." *J Colloid Interface Sci* 304 (1):119-24. doi: 10.1016/j.jcis.2006.08.055.